ISSN 8755-6839

SCIENCE OF **TSUNAMI HAZARDS**

Journal of Tsunami Society International

**Volume 36** **Number 4** **2017**

# THE 7.8 $M_w$ EARTHQUAKE AND TSUNAMI OF 16th April 2016 IN ECUADOR: Seismic Evaluation, Geological Field Survey and Economic Implications

**Theofilos Toulkeridis[1]*, Kervin Chunga[2], Willington Rentería[3], Fabian Rodriguez[1,4], Fernando Mato[1], Sissy Nikolaou[5], Mario Cruz D´Howitt[1], Davide Besenzon[6], Hugo Ruiz[1], Humberto Parra[1] and Xavier Vera-Grunauer[7,8]**

[1]Universidad de las Fuerzas Armadas ESPE, Sangolquí, Ecuador
[2]Universidad Estatal Península Santa Elena, Facultad de Ciencias de la Ingeniería, La Libertad, Ecuador.
[3]Instituto Oceanográfico de la Armada del Ecuador (INOCAR), Guayaquil, Ecuador
[4]Pontificia Universidad Católica del Ecuador (PUCE), Facultad de Economía, Quito, Ecuador
[5]WSP Parsons Brinckerhoff, New York City, USA
[6]Escuela Superior Politecnica del Litoral, Facultad de Ingeniería en Ciencias de la Tierra, Guayaquil, Ecuador
[7]Facultad de Ingeniería, Universidad Católica de Santiago de Guayaquil (UCSG), Guayaquil, Ecuador
[8]Geoestudios, SA, Guayaquil, Ecuador

*Corresponding author: ttoulkeridis@espe.edu.ec

## ABSTRACT

We evaluated the recent earthquake and tsunami responsible for considerable damage and 663 deaths due to a 7.8Mw movement on the 16th of April 2016. The seismic event filled tens of thousands in refugee camps and affected some two million persons directly. The potential of high losses and damage with a total of 29,672 properties, including family houses, is also given by the fact that the infrastructure of the fishing, tourism and other industries and the movement to live along the beaches, have been highly developed within the last decades along the Ecuadorian coasts. The geological survey and determination of field data were performed three days after the main seismic event, allowing to obtain 290 data coseismic effects on the ground that allowed to evaluate the maximum macroseismic intensities as well as the predominant geomorphological features.The results of these sampling stations allowed to reconstruct a geological map with isoseismals fields of intensities. With

all the compiled and recorded coseismic data in the field of higher macroseismic intensities, we proceeded to produce a map of intensities applying the definitions and degrees of the ESI 2007 scale. We also evaluated the distribution and intensities of the aftershocks demonstrating the spatial-temporal affinities. The occurred tsunami, although less destructive than previous in the same region has been documented with all details available.

The economical assessment included in this study concludes that this earthquake impacted a large part of a variety of coastal cities destroying between 70 and 80% of some close-by villages and cities with a distance of 140-150 km of the epicenter, which suffered damages of their buildings within 40 to 55%, in which lines of electricity transmission, infrastructure of water supply, hospitals, schools, private and public buildings, main roads and highways have been severely affected or even completely destroyed. The costs of the damages of the mentioned infrastructure are summing up an approximate loss of some 3.3 billion USD, being equivalent to 3.31 % of the Ecuadorian GDP. In addition to losses in infrastructure and properties, over 28 thousand jobs were lost and about 300 million US$ in trade and businesses.

**Keywords:** *Earthquake, Tsunami, seismic damage, economic losses, Ecuador*

## 1. INTRODUCTION

The deadliest of all natural hazards by death toll are earthquakes along with their secondary affects like tsunamis (Kahn, 2005; Anbarci et al., 2005; Raschky, 2008; Marano et al., 2010; Holzer and Savage, 2013). The recurrance of seismic events has been ~~studied~~ extensively ~~by~~ researched (e.g., McGuire, 1995; Shome et al., 1998; Ruff and Kanamori, 1980; McCaffrey, 2008). Earthquakes also generate tsunamis, either being in or close to masses of water, like lakes, seas or oceans, generating landslides or other types of massive mass movements or failures (Gutenberg, 1939; Pararas-Carayannis, 1967; Synolakis et al., 2002; Bardet et al., 2003; Gusiakov, 2005; Tinti et al., 2005; Pararas-Carayannis, 2006; 2010; 2012; 2014; Bryant, 2014). There is at least a dozen of known earthquakes and subsequent tsunamis that have claimed more than 100,000 lives. Among these, two single events in China caused more than 700,000 human losses (Butler et al., 1979; Chen, 1988; Gang, 1989; Hou et al., 1998; Gupta et al., 2001), and the 2004 seismically-induced tsunami claimed some 280,000 lives in Indonesia and neighbouring countries (Sieh, 2005; Ghobarah et al., 2006).

In Ecuador, around one dozens of tsunamis have been generated during the past two centuries, close-by or above the Colombian-Ecuadorian trench within the existing geodynamic setting shown on Fig. 1 (Berninghausen, 1962; Kanamori and McNally, 1982; Pararas-Carayannis, 2012). Moreover, recent bathymetric mapping detected submarine landslide scars of a steep-sided fracture zone named "Yaquína Fracture Zone" shown on Fig. 2, that is certainly capable of generating tsunamis (Collot et al., 2004; 2005; 2010; Ratzov et al., 2007; Collot et al., 2010; Ioualalen et al., 2011).

The focus of this paper is the evaluation of the $M_w$7.8 earthquake on the 16$^{th}$ of April 2016, which caused hundreds of deaths and considerable damage and generated a tsunami detected during its movement along the Ecuadorian shores.

## 2. GEODYNAMI SETTING OF ECUADOR AND SEISMOGENIC ORIGIN

Due to its geodynamic situation along the Pacific Rim, the coastal Ecuadorian continental platform is often the target of earthquake activity and subsequent tsunamis (Gusiakov, 2005; Pararas-Carayannis, 2012; Rodriguez et al., 2016). The active continental margin and associated subduction zone between the oceanic Nazca Plate with the continental South American and Caribbean Plates (Fig. 1), both separated by the Guayaquil-Caracas Mega Shear (Kellogg and Vega, 1995; Gutscher et al., 1999; Egbue and Kellog, 2010) give rise to tsunamis of tectonic, as well submarine landslide origin (Shepperd and Moberly, 1981; Pontoise and Monfret, 2004; Ratzov et al, 2007; 2010; Ioualalen et al., 2011; Pararas-Carayannis, 2012). The main seismic source in the Ecuadorian territory is the subduction zone, which is about 756 kilometers (km) long, at a distance between 60 and 150 km from the coastline of continental Ecuador.

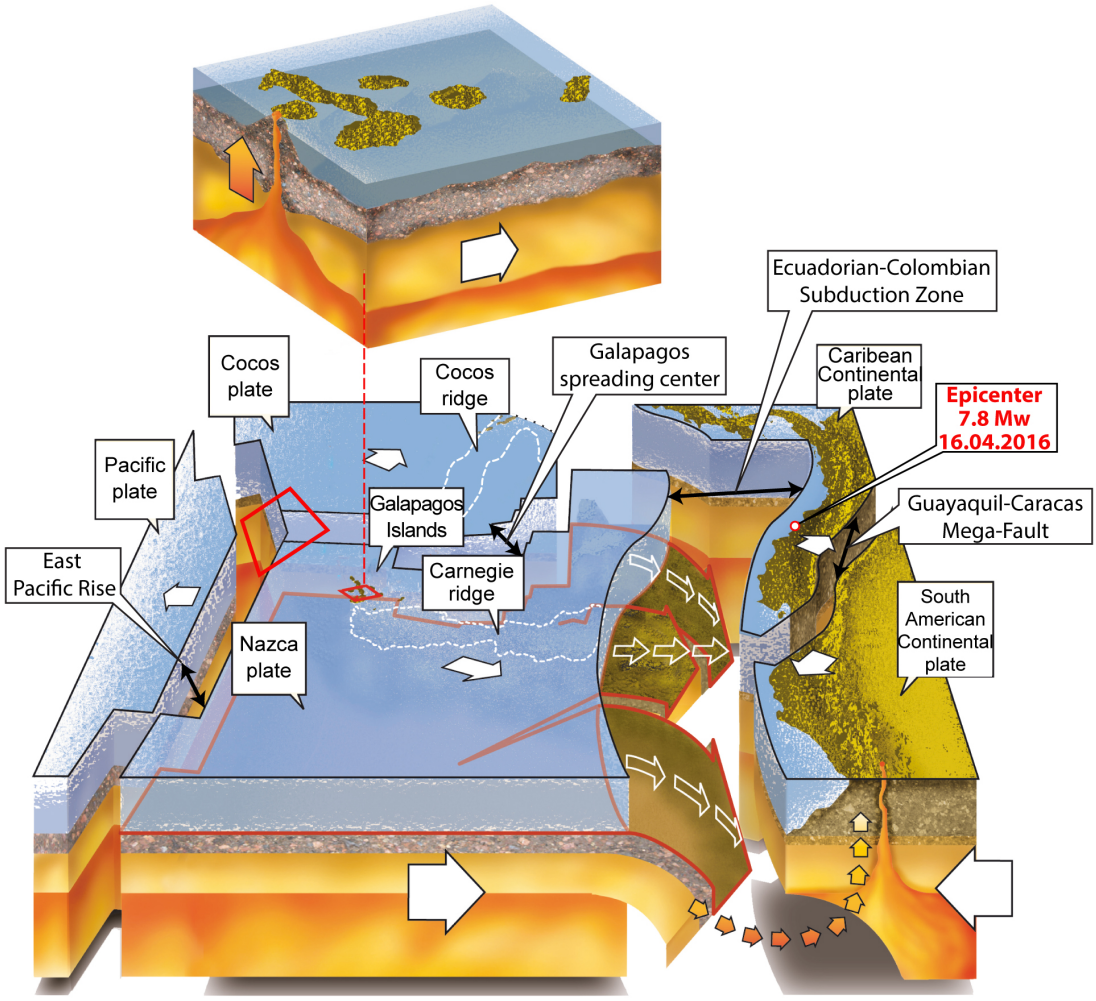


Fig. 1: Geodynamic setting of Ecuador, the Galapagos Islands and the Carnegie Ridge. Adapted from Toulkeridis, 2013 and Rodriguez et al., 2016.

Another origin of earthquakes and tsunamis has been credited to the Galápagos volcanism (Toulkeridis, 2011). The active Galápagos hotspot has produced several voluminous shield-volcanoes, most of which are inactive due to the ESE-movement of the overlying Nazca oceanic plate (Holden and Dietz 1972; Toulkeridis, 2011). The main Galápagos Islands are located south of the EW-trending Galápagos Spreading Center, east of the NS-trending East Pacific Rise, and approximately 1,000 km west of the Ecuadorian mainland.

The volcanic activity and subsequent plate drifting have generated two aseismic volcanic ridges: (i) the Cocos Ridge moving NE above the Cocos Plate and (ii) the Carnegie Ridge moving East above the Nazca Plate (Harpp et al., 2003). These submarine extinct volcanic ridges are the result of cooling/contraction reactions of magma, as they slowly sunk below the sea surface due to lack of magma supply, lithospheric movement and strong erosional processes (Fig. 1). With time, these ridges, as well as various microplates, have accreted on the South American continent (Reynaud et al., 1999; Harpp and White, 2001).

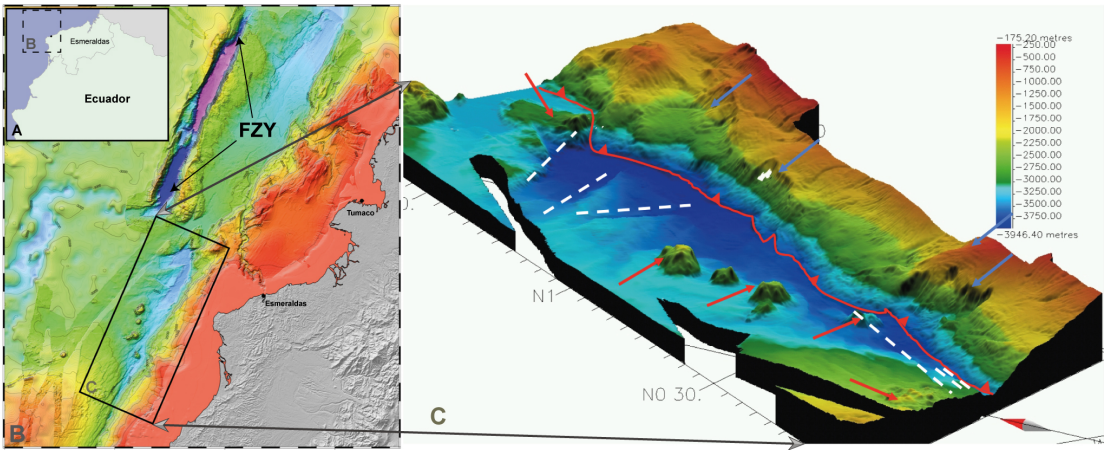


Fig. 2: (a) Detailed morphology of continetal rim of NW Ecuador. Inlet (b) shows the Fracture Zone of Yaquina (FZY) extension, and (c) highlights geodynamic aspects, such as deformation front between Nazca Oceanic and Carribean Continental Plates (red line), active faults at oceanic crust floor (white dashed lines), seamounts entering the subduction zone (red arrows), and scars of landslides, fissures and submarine debris (blue arrows). Adapted from Collot et al., 2010.

Nonetheless, such aseismic ridges, like Carnegie Ridge, may become an obstacle in the oblique subduction process by generating a potential valve of marine quakes within the subduction zone with earthquakes and occasionally tsunamis along the Ecuadorian coast (Pararas-Carayannis, 2012). The Carnegie Ridge collides towards the Ecuadorian continental margin with an average velocity of 5 cm/year at a latitude between 1°N and 2°S (Pilger, 1983).

From historic records of the last two centuries, the Ecuadorian shoreline has experienced strong, locally-generated earthquakes and marine quakes, with occasional triggering of tsunamis. On of these events was the great earthquake of 1906 with estimated $M_w$8.8 and 600-km long rupture area

(Rudolph and Szirtes, 1911; Kelleher, 1972; Beck and Ruff, 1984; Kanamori and McNally, 1982; Swenson and Beck, 1996; Pararas-Carayannis, 2012), with scarce evidence of paleo-tsunami deposits (Chunga and Toulkeridis, 2014). Other earthquakes with subsequent tsunamis along the Ecuador–Colombia subduction zone include the tsunamis of 1942 ($M_w$7.8), 1958 ($M_w$7.7) and 1979 ($M_w$8.2) within the 1906 rupture area (Collot et al., 2004). While the 1906 event caused the death of up to 1,500 persons in Ecuador and Colombia with an unknown financial damage to the existing infrastructure, the 1979 tsunami killed at least 807 persons in Colombia and destroyed approximately 10,000 homes, knocking out electric power and telephone lines (Pararas-Carayannis, 1980; USC&GS, 2016a).

Evaluation of the last marine quakes which generated tsunamis, suggests that the probability of a major or great earthquake in this margin region is highly likely, especially as there appears to be substantial strain accumulation in this region (Pararas-Carayannis, 2012). Considering that the last earthquake in 1979 did not release the amount of energy of the 1906 event, there is a high calculated probability of a tsunami of similar magnitude to that of 1906 in the near future, due to a potential earthquake within the Ecuadorian-Colombian trench. Based on historic evidence of tsunamis in Ecuador from the last 200 years, the estimated probability of a strike in 2015 reached 87% (Rodriguez et al., 2016). A potential future tsunami may be even more destructive than the one in the past if it occurs near high tide (Pararas-Carayannis, 2012). The risk exposure is greater since, in the last decades, the population density has increased along the shorelines and the infrastructure of the major industries of fishing and tourism is also concentrated along the shores.

## 3. GEOLOGICAL AND TECTONIC SETTING OF THE EPICENTRAL AREA AND IMPLICATIONS FOR SEISMIC WAVES

The rock deposits from Pedernales to Bahia de Caraquez are represented by tertiary geological formations (Oligocene to Miocene), with some minor recent rock formations like the Onzole and Borbon being of the Pliocene. The Dos Bocas and Villingota units belong to the Tosagua formation are the oldest sedimentary rocks in the epicentral area of the 2016 earthquake besides the basaltic basement. The Dos Bocas formation consists of brown, well stratified hard shales, with interbedded siltstones and fine to medium-grained sandstones, with minor thin abundant gypsum veinlets being fractures filling as well as thin sandstone and dolomite layers. This stratigraphic sequence is followed by the younger lithologic units of the Villingota Formation, which consists of thin layers of gray tuffaceous shales, being interbedded with some medium-grained yellow sandstones (Bristow and Hoffstetter, 1977; Baldock, 1982).

Rock appears broadly in the epicentral area and is well evident in slopes of hills of San Vicente and Bahia de Caraquez that have origin of the Onzole Formation (Stainforth, 1948). They consist of laminated siltstone interspersed with fine layers of sandstones and fracture fillings of gypsum. Some of the siltstone in the Onzole formation is underlying sandstones of the Borbon formation, while the base of the crust correspond to the Cretaceous basaltic formation of Piñon (Tschopp, 1948; Bristow y Hoffstetter, 1977; Feininger, 1980; Lebrat et al., 1987).

The Digital Terrain Model (DTM) interpretation of Fig. 3 demonstrates the existence of pronounced system of reverse faults with NNE-SSW directions, characterized by a component of dextral transcurrent. Possibly this system is related to the compressional forces acting on the coast, where clastic sedimentary rocks are dominant (Reyes and Michaud, 2012). In the study area, the faults observed do not evident NW-SE directions, except for a block located between Pedernales and Canaveral, limited by older regional faults of NNW-SSE directions that have been intersected by the predominant NNE-SSW fault system.

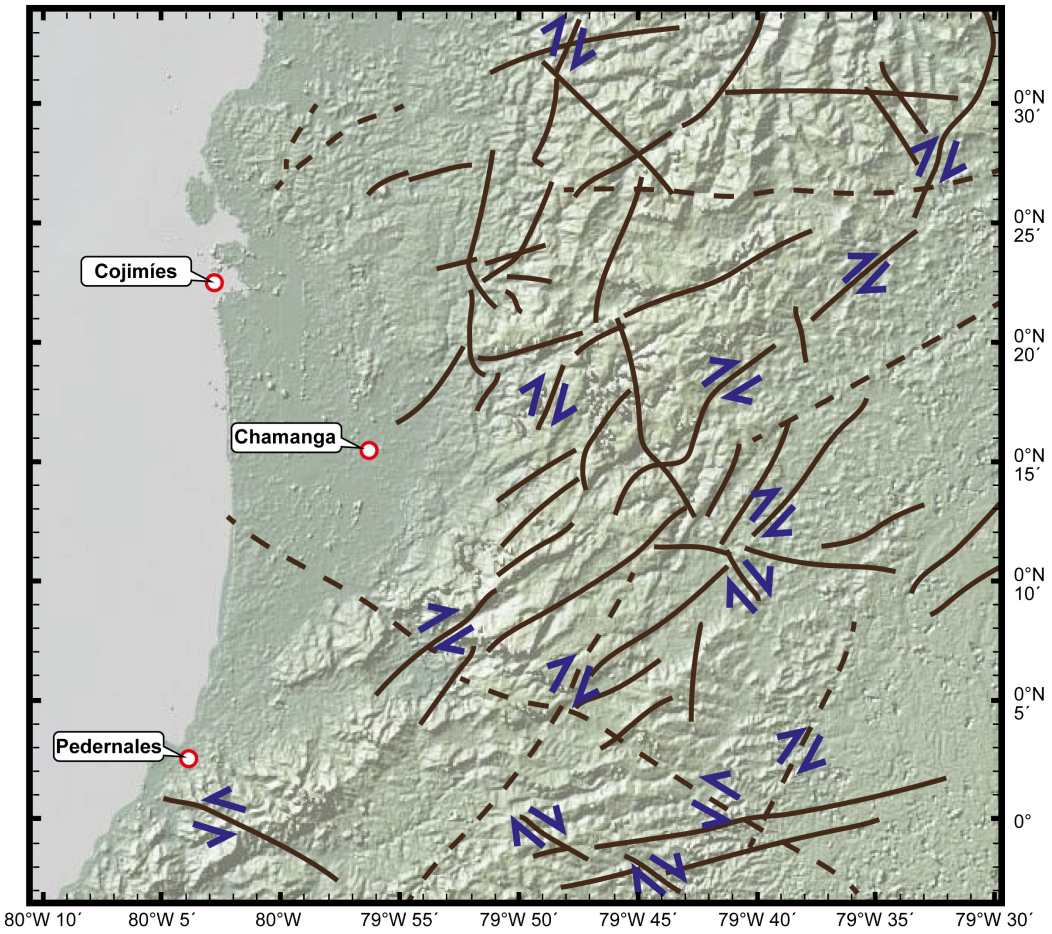


Fig. 3. Digital Terrain Model (DTM) with the schematic tectonic analysis of the Cordillera Costanera in the section Pedernales - Cojimíes.

The propagation of seismic waves differs in the various rock types, depending mainly on their stiffness and lithological consistency and thickness. Moreover, site amplification effects may be generated as the waves propage through the Holocene sediments (Sato et al., 2012). Geomorphologically, the epicentral area is formed by the supratidales coastal plains, areas of depressions between hills, plains of paleo-meander floodplain which can affect the intensity of the ground motions from both a topographic and geologic perspective (Chunga et al., 2016; Papanikolaou et al., 2010).

Watersheds of the coastal region of Manabi are characterized by alternating periods of erosion and sedimentation, with frequent alluvial fans deposited on hill tops. One of the main river structures is the basin of Portoviejo that is occupied by many villages. This basin is filled over time with soft or loose deposits (typical of Class E or F sites as per international codes) that may amplify the motion or become unstable or lose strength during a seismic event (Chunga et al., 2016). Regional seismic hazard studies have considered the geomorphological position of the watershed-axis and the direction of the seismogenic structure, and demonstrated that wave attenuation may be less prominent in the area of low-compacted alluvial deposits. The orientation of the watershed in the Manabi Province is heading from east to west, which is an unfavorable for the potential seismic effects.

## 4. THE EARTHQUAKE OF 16th APRIL 2016

In the late afternoon of Saturday, at 18:58:36 (UTC-05:00) local time, an earthquake with moment magnitude of $M_w$7.8 impacted the coastal Ecuador (Fig. 4) with epicenter 29 km SSE of the town of Muisne in the Esmeraldas province (Lat.: 0.353ºN; Long.: 79.925 ºW; USGS, 2016b), and hypocentral depth of 21 km. The event took the life of 663 people, moved tens of thousands in refugee camps and directly affected the lives of 2 million persons.

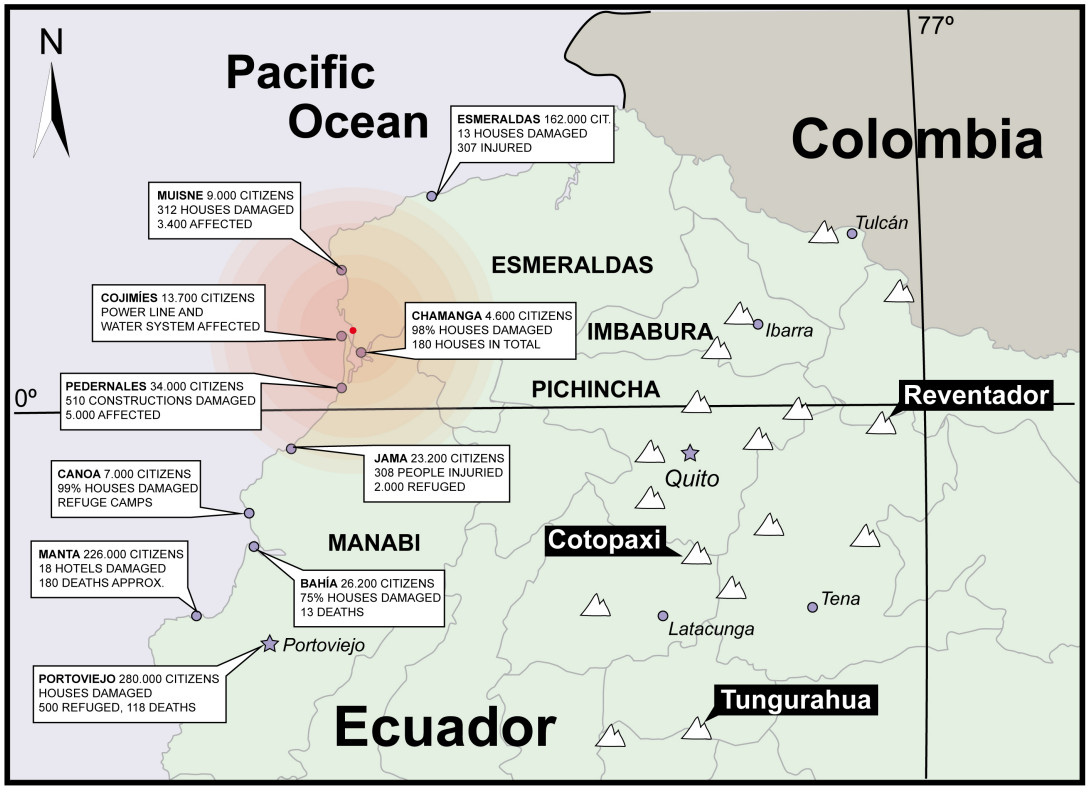


Fig. 4: Epicenter of the $M_w$7.8 earthquake (red dot) and selected damage observations in several coastal cities.

This earthquake has, in many aspects, similarities with the estimated $M_w$7.8 earthquake of May 14$^{th}$, 1942, but the tsunami triggered by a submarine landslide or coseismic deformation did not have significant impact. However, if in the future the epicentral area is within the continental margin and the macroseismic intensity is higher than IX, it is likely to find evidence of underwater landslides (Michetti et al., 2007).

The earthquake impacted a large portions of several coastal cities, destroying between 70 and 80% of nearby villages and cities, Pedernales, Jama and Canoa (area of maximal macro-seismic intensities of IX to X), and cities within a distance of 140-150 km from the epicenter, like Chone, Portoviejo and Manta, which suffered building damage within 40 to 55%. As shown on Fig. 4, lines of electricity transmission, infrastructure of water supply, hospitals, schools, private and public buildings, main roads and highways were severely affected or completely destroyed. The cost estimate of the damage in the building stock and infrastructure were estimated at 3.3 billion USD (El Telegrafo, 2016; SENPLADES, 2016).

The mainshock was followed by 84 aftershocks with moment magnitude $M_w$ between 3.8 and 6.8, recorded by the USGS in Ecuador (and hundreds by the IGEPN) until May 20$^{th}$. The highest magnitudes were registered around the rupture zone with 86% of them during the first 10 days after the main shock (Toulkeridis et al., 2016; Tierra et al., 2017).

## 5. STATISTICAL EVALUATION AND GEOPHYSICAL CLUSTERING OF THE MAIN EARTHQUAKE AND AFTERSHOKS

A thorough understanding of the regional tectonics and the modeling of the rupture point to the second plane are essential in gaining insight to how the earthquake was generated. On the one hand, the earthquake occurred in an area where the subducting Nazca plate under the Caribean plate slides at a rate of 61 mm/year (Fig. 1). The focal mechanism of the main earthquake was a reverse fault with nodal planes given by the triads (strike, dip, rake) equal to (183°, 75°, 84°) and (26°, 16°, 113°) as reported by USGS (USGS, 2016b).

The location and mechanism are consistent with a subduction earthquake interface, sliding over an area approximately 160 km long and 60 km wide. On the other hand, the main earthquake was followed for weeks by a large number of seismic events generated (IGEPN, 2016a) , 678 of which were registered within the affected area until May 20$^{th}$ (IGEPN, 2016b) as shown on Fig. 5a. A large portion of these registered events, of about 88%, were not directly related to the rupture zone (USGS, 2016c), as indicated in Fig. 5b (USGS, 2016d). Furthermore, the spatial location uncertainty of the afterschocks reported by IGEPN (Figs. 5a, 6a,b, IGEPN, 2016a,b) dificults the study of the geodynamics of the subduction process (Fig. 7a), masking the existence of three distinct seismic clusters in such process (Fig. 7b): (1) Zone 0 (red), around Muisne; (2) Zone 1 (green) around Bahía Caraquez; and (3) Zone 3 (blue) around Manta.

The presence of such clusters has been demonstrated previously (Toulkeridis et al., 2016), by correlating the discovery of a clear pre-seismic environmental radiation with the spatio-temporal

distribution of the USGS records. The methodology followed allows, with respect to the rupture process: (1) the association of seismic events with the main points of energy release; (2) a geophysical clustering of aftershocks; and (3) the identification of the geodynamic relationships between clusters since the time of the main shock.

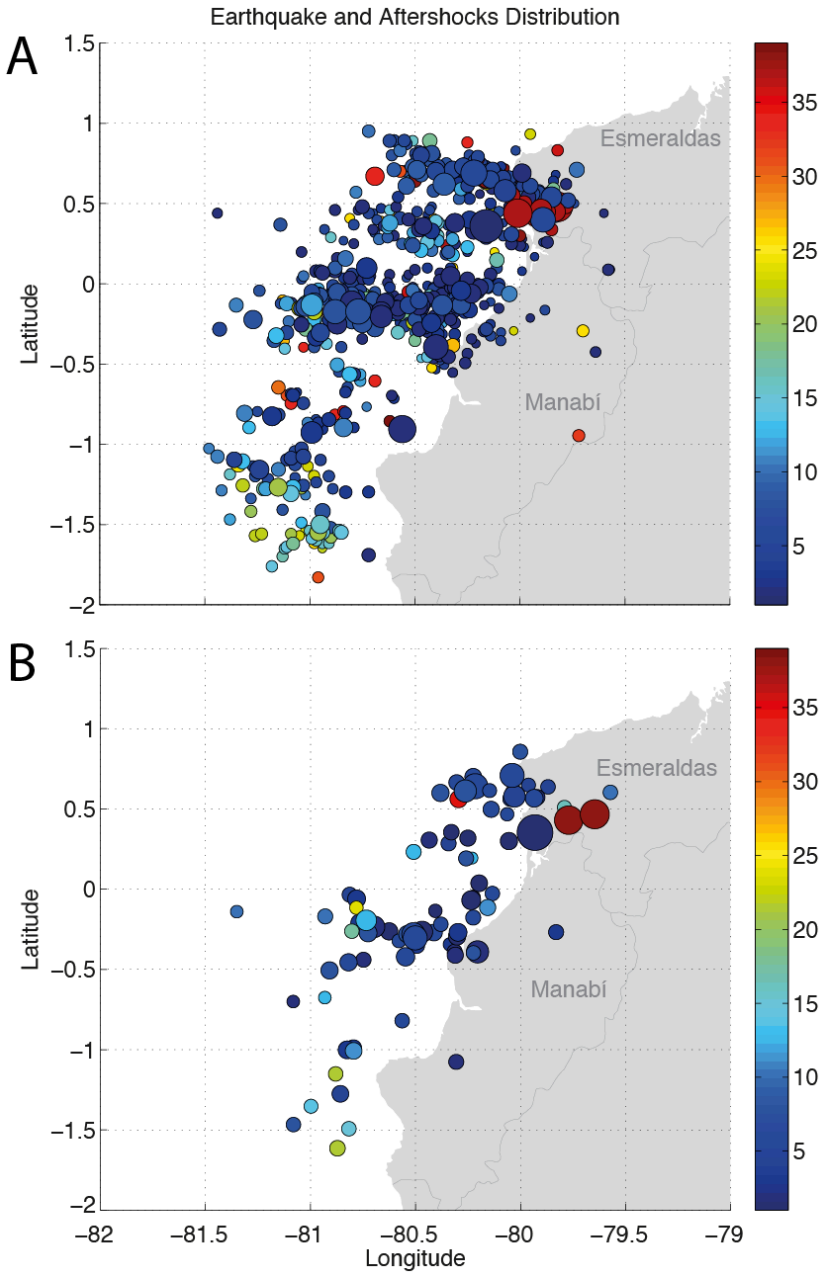


Fig. 5: Spatio-temporal distribution of the April 16, 2016 $M_w$7.8 Muisne, Ecuador Earthquake and aftershocks registered by IGEPN (a) and USGS (b) within the affected area [79.5W - 81.5W, 2S - 1N] from April 16$^{th}$ (dark blue) to May 20$^{th}$ (dark red).

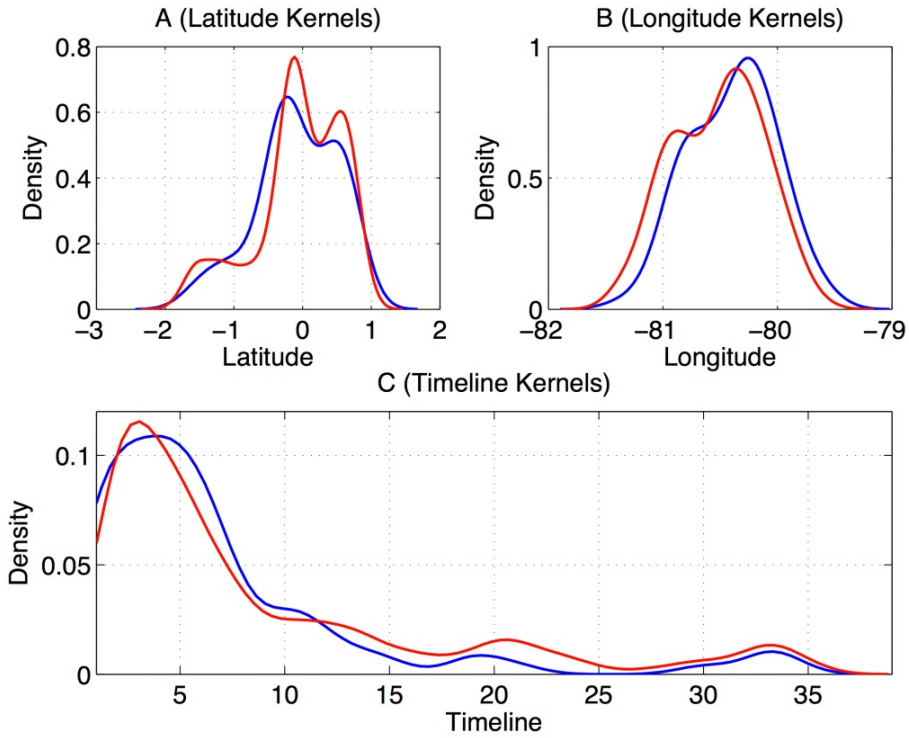


Fig. 6: Latitude (a) and Longitude (b) kernels distribution of the April 16, 2016 $M_w$7.8 Muisne, Ecuador Earthquake and aftershocks registered by IGEPN (red) and USGS (blue) within the affected area [79.5W - 81.5W, 2S - 1N]; (c) corresponding timeline kernels distribution. , Observations presented up to May 20$^{th}$2016.

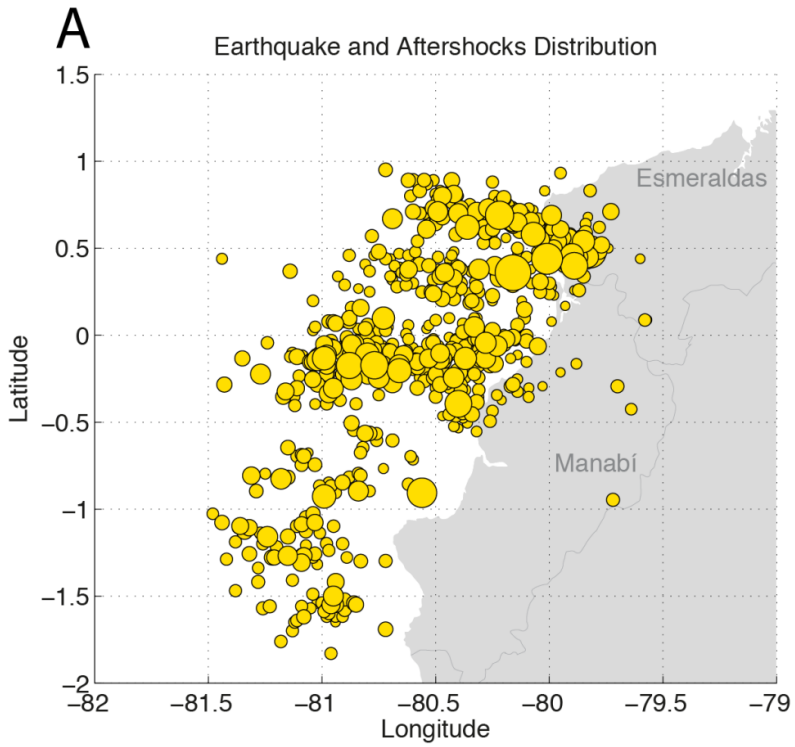

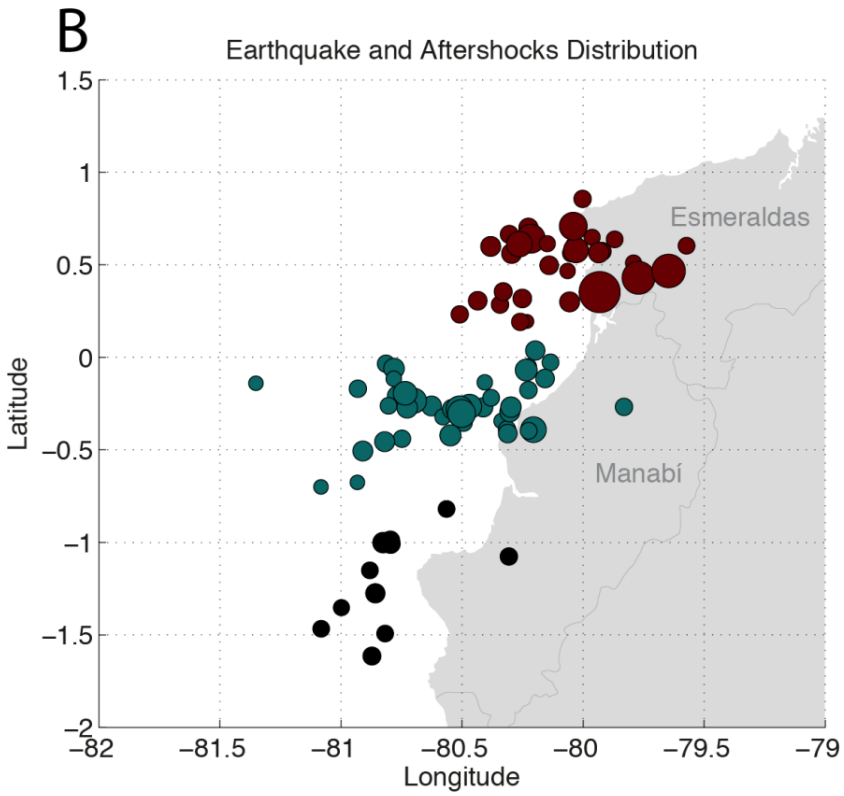


Fig. 7: (a) Spatial distribution of the April 16, 2016 $M_w$7.8 Muisne, Ecuador Earthquake and aftershocks registered by IGEPN; (b) geophysical clustering by means of the pre-seismic environmental radiation correlation with the spatio-temporal distribution of USGS data (Toulkeridis et al., 2016). Observations presented within the affected area [79.5W-81.5W, 2S-1N] up to May 20th, 2016.

## 5. SEISMIC HAZARD EVALUATION BASED ON THE CO-SEISMIC GEOLOGICAL DAMAGES

The geological survey and field data collection was performed within 3 days from the main seismic event, providing 290 data points of coseismic effects on the ground that allowed to evaluate the maximum macroseismic intensities and the predominant geomorphological features. The latter are important in evaluating site effects documented in Muisne, Pedernales, Jama, Canoeing, Chone, San Isidro, Manta, Portoviejo and Tosagua.

Aftershocks with $M_w$ of 6.8 (02:57 a.m. local time) and 6.9 (11:46 a.m.) were recorded on May 18th, 2016, with hypocentral distance of 15 km. These events are associated with the same seismogenic structure responsible for the main $M_w$7.8 event and generated effects such as sinkholes, soil liquefaction with sand ejecta in Muisne and minor landslides in Pedernales and Mompiche. We evaluated the intensity through observations of damage to the environment, applying the macroseismic intensity scale ESI 2007 (Environmental Seismic Intensity; Michetti et al., 2007).

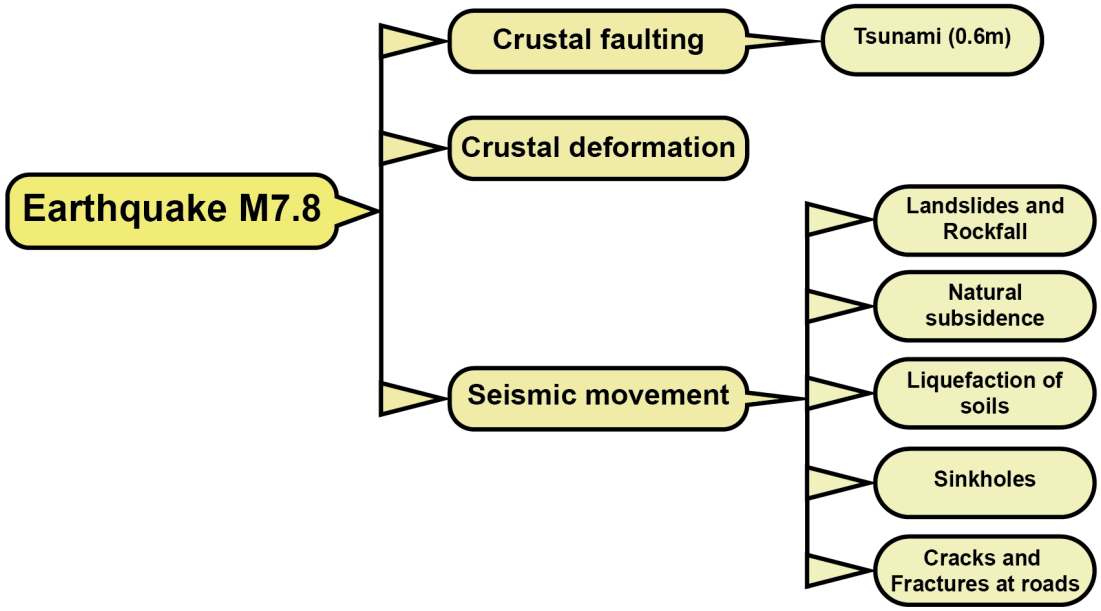


Fig. 8: Primary and secondary effects during and following the main $M_w$7.8 earthquake (Chunga et al., 2016).

In order to understand the isoseismal fields of macroseismic intensities and delineate the epicentral area of the main earthquake, the coseismic geological information has been compiled in the field based on (see Fig. 9): (a) landslides of natural and stabilized slopes, (b) cracks in natural field in the supratidal coastal plains and flood plains, (c) longitudinal and transverse fractures to the main axis of the concrete and paved roads, (d) sinkholes and soil liquefaction (e.g., sand ejecta and boils) formed in floodplains and areas of paleo-meander, (e) surface faulting with vertical and horizontal displacements (i.e., dextral shears) in hilly areas, (f) natural and anthropic subsidences in areas of depressions between hills and floodplains, (g) minor tsunami formed in the ocean with logs of a run-up height of less than 1 m. Field effects have been incorporated when the local seismic intensity is higher than VI. The implementation of the ESI 2007 scale (Michetti et al., 2007) has allowed to assign intensities based on evident ground effects in the different geomorphological settings of the Manabi and southern Esmeraldas provinces.

### 5.1 Geological mapping of features corresponding to an intensity of IX

Seismic effects in the epicentral area based on geomorphological features of supratidales coastal plains, floodplains, coastal terraces and depressions (filled areas) and between hills (Jama) were mapped. The supratidal areas experience wavy surface deformations, affecting buildings and streets (Figs. 9, 11). Some cobblestones were re-arranged as folds with vertical displacements from 8 to 10 cm recorded in Pedernales. Subsidence of cobblestone layers were commonly observed as shown on Fig. 10.

Fig. 9: Deformations along concrete-made road between Pedernales and Coaque, with diagonal and transverse fractures 10 to 14 cm wide. geomorphological floodplain features. ESI Intensity of IX and coordinates (UTM: 602.858mE 10.003.638mN).


Fig. 10: Wavy deformations on the beach boardwalk and streets of Pedernales, with re-arrangements of cobblestones in folds. ESI Intensity of IX to X and coordinates (UTM: 604.756mE 10.007.656mN).

Visible damage of the concrete road between Pedernales and Coaque included uplift internal steel beams that formed transverse fractures with openings of 8-15 cm (Fig. 9). In paved roads, the deformations generated bigger fractures, reaching 20 to 30 cm openings within transverse esruptur (Fig 11; Jama, UTM Coord. 584.676mE, 9.982.122mN.).

Fig. 11: Deformation in Jama paved road, with transversal fractures 20 to 30 cm wide and longitudinal fractures of 12 to 15 cm. Cracks observed in the free field soils reached 1 m. ESI Intensity of IX and coordinates (584.676mE 9.982.122mE).

In the natural terrain or soil of this area, crack openings reached 1 m. Such deformation characteristics were also observed in Pedernales and Coaque, but not towards the north, in Cojimies and Chamanga, confirming that the earthquake was felt strongly towards the south of the epicenter. In some other sites, the land appeared to have settled with apparent evidence of liquefaction in flooded areas and sand ejecta as shown on Fig. 12.

Fig. 12: Liquefaction evidence from GEER helicopter flyover of Manabí coast (Nikolaou et al., 2016), close to Jama (0º12'31.7"S, 80º15'22.5"W UTM coordinates 9976918.8N, 582762.5E).

### 5.2 Geological mapping of features corresponding to an intensity of VIII

Landslides and rockfalls of natural slopes were evident throughout the affected area (Fig. 13) with 126 reports out of 290 sampling stations. Stabilized slopes also reported damages in the epicentral area (Fig. 14), like in the northern side of Canoa, where part of a slope was deformed with a displacement escarpment. Field inspections indicated that the slope was likely not adequately stabilized, since the top did not have any stabilization work done and presented cracks and fissures with water runoff (Fig. 15).

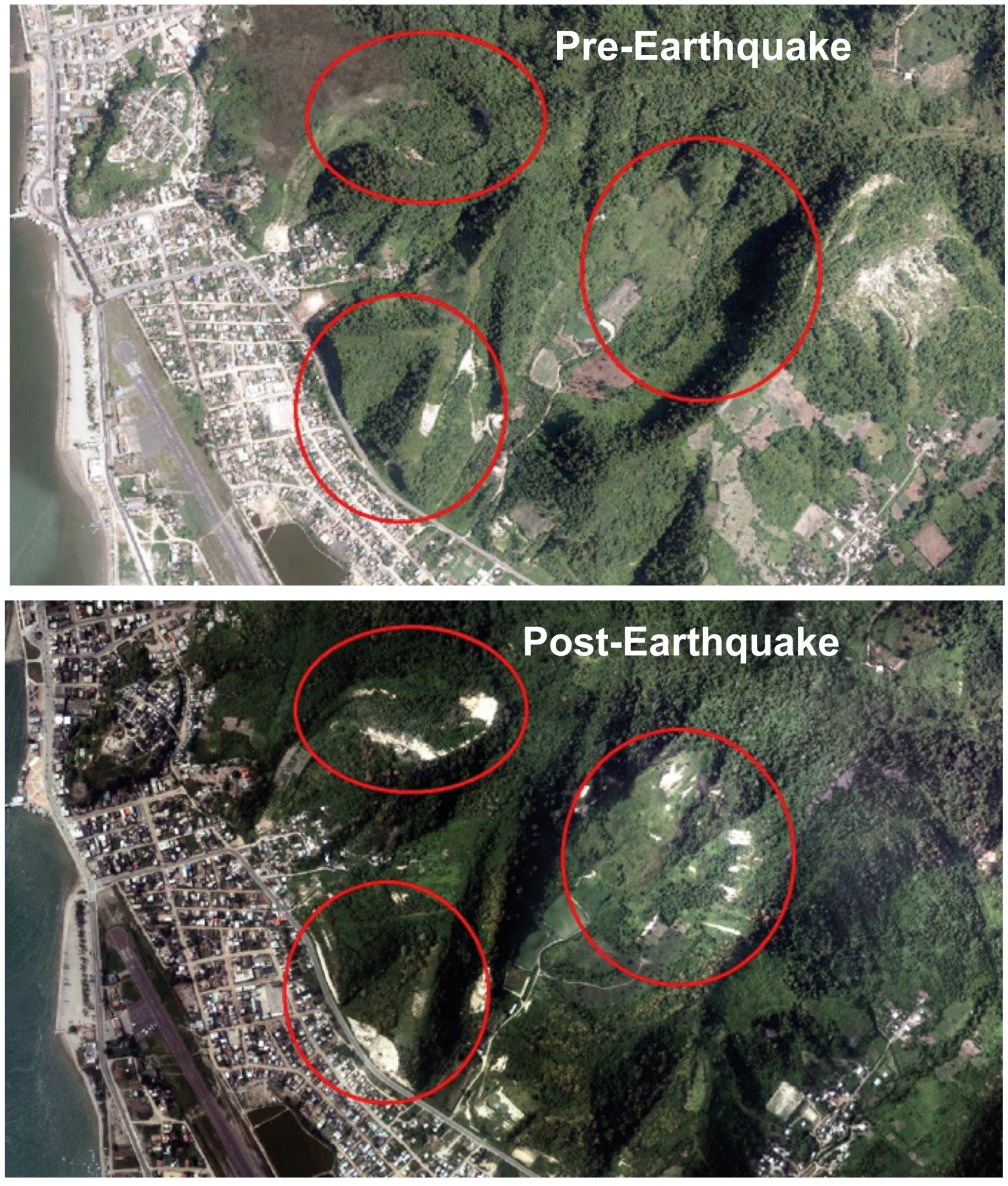


Fig. 13: Satellite images of pre- and post-earthquake. In the hilly area of San Vicente, the displacement rate of active landslides was increased during the main earthquake. This hazard area may be re-activated during winter periods with high rainfall. Intensity ESI = VIII. Images courtesy of the Military Geographical Institute of Ecuador.

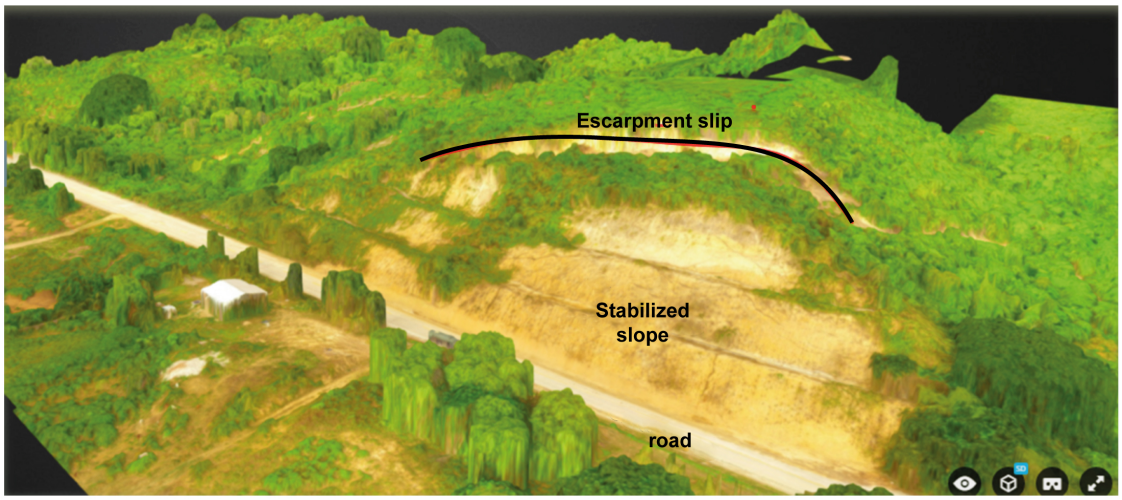


Fig. 14: Digital Terrain Model (DTM) from drone images, showing rotational slip on the road El Rosario - Canoa. Courtesy: Global Medical – SGR. Intensity ESI = VIII and coordinates (UTM: 561.268mE 9.952.722mN).


Fig. 15: Rotational slip in the road El Rosario – Canoa with evidence of escarpment at the slope and damages on the bicycle path and concrete road. Approximately 400 $m^3$ of material slipped (Chunga et al, 2016.). ESI Intensity = VIII and coordinates (UTM: 561.268mE 9.952.722mN).

In the accumulation zone at the lower part of some slopes, we documented between 800 to 10,000 $m^3$ of colluvium and debris, which affected some rails of the main paved and concrete roads. Rotational landslides in the filled areas between sections of slopes triggered lateral spreading. In the area of Boca de Briceno, the rocky mass of the hills showed fracturing or active jointing resulting to rock falls.

Fig. 16: Aerial photo of landslide on San Vicente-Canoa local road by GEER (Nikolaou et al., 2016). (GPS: 0°33' 5"S, 80°25'42"W UTM coordinates 9939051.9N, 563610.3E)

Fig. 17: Massive rockfall, which covered and destroyed completely the paved road with some 10,000 $m^3$ at Boca de Briceño. Intensity ESI = VIII, coordinates (561.647mE 9.944.416mN).

In the epicentral area, rock falls occurred in slopes of hills and filled areas or depressions between hills. Longitudinal, diagonal or transverse fractures of up to 25 cm were reported in Coaque, Jama and Canoes, San Isidro, Ricaurte, Bahia de Caraquez, Flavio Alfaro, Boca de Palmito, Pavon, Marco and San Clemente (Figs. 16 to 18). The sites farthest from the epicenter, but within the Manabi province, also reported multiple slides. In Esmeraldas, similar damage occured in Mompiche, Salima, Daule, Bellavista and Chamanga.


Fig. 18: Transcurrent displacement of ~35 cm on the paved road between San Vicente-San Isidro. Intensity ESI = VIII , coordinates (UTM: 573.419mE, 9.939.274mN).

In Crucita, vertical settlements and lateral deformations due to instability may be attributed to liquefaction, although surface manifestation of sand ejecta was not identified in reconnaissance. The assumed failure planes on Fig. 19 appear to be either along the interface between the embankment and the foundation soils (planar surface), or through the foundation soils. The latter, indicative of a more circular surface failure, may be due to liquefaction-induced softening that allowed the reduced-strength soil to shear during the earthquake (Nikolaou et al., 2016).

In Chamanga, several homes collapsed with evidence of 15-25 cm wide cracks due to lateral deformations in the supratidal coastal zone (Fig. 20) and bearing failures. In total we documented 65 sites in the cities and towns of Cojimies, Pedernales, Coaque, Jama, Canoeing, San Vicente, Bridge Mejia, Junin, San Isidro, Chone, Manta, Rocafuerte and Chamanga with similar damage patterns.


Fig. 19: Aerial view of embankment failure with assumed movement and failure modes marked with yellow at Mejia Bridge. Coord. UTM: 558.990mE 9.890.563mN. Intensity ESI = VIII. GEER-ATC report (Nikolaou et al., 2016).

Fig. 20: In Chamanga cracks in natural terrain with openings of 15 to 25 cm and collapses of buildings. Intensity ESI = VIII.Coordinates UTM: 616034mE 10009804mN.

Furthermore, soil liquefaction and sinkholes were observed along with sand boils in Muisne, Boca de Briceno and Tosagua (Figs. 21 to 24). The soil profile in these areas consists of sedimentary features formed in active and abandoned floodplains as well as paleo-surface meanders, which is combined with shallow ground water table. Observations of lateral spreading at river banks and road cuts on slopes included crack openings of up to 30 cm. In the central park of the island Muisne, a variety of sand boils (Figs. 17 and 18) between 50 cm to 80 cm in diameter were formed 1 minute after the main $M_w$7.8 earthquake, submerging two blocks of the park and leaving behind wavy deformation patterns in sidewalks, cobbles and streets. Similar phenomena were re-activated during the strong aftershocks of May 18$^{th}$, 2016 (11:46 a.m) that reached $M_w$ of 6.8.

Fig. 21: Liquefaction evidence in the central park of Muisne Island. Intensity ESI = VIII and coordinates (UTM: 609170mE 10067485mN).


Fig. 22: Sand boils with a diameter of 30 to 55 cm. 585364mE 9913357mN. Intensity ESI = VIII.

Fig. 23: Boca de Briceno Bridge liquefaction evidence in free-field and adjacent to embankment footing from GEER observations (Nikolaou et al., 2016) (GPS: 0°30'59"S, 80°26'31"W) UTM coordinates 9942920.8N, 562096.1E.


Fig. 24: Sinkhole at Tosagua village site with diameter of 2-3 m within floodplain and evidence of subsidence. Tosagua has been settling above an abandoned meander plain.

### 5.3 Geological mapping of features corresponding to an intensity of VII

From the 290 sampling stations, 73 had evidence of mass movements of landslides and rockfalls of natural slopes. The volume of accumulated material from unstable natural slopes has been estimated on the order of 50-250 $m^3$. In San Vicente, fallen rocks reached up to 1 m in diameter. On the slopes via San Isidro (UTM coordinates 586.049mE, 9.960.532mN), we documented the tree layer denudation phenomenon. Geomorphological features where these landslides effects were observed are in slopes and roadcuts of alluvial terraces at sites in Coaque, Jama, Canoeing, San Vicente, San Jacinto, Portoviejo, Pueblo Nuevo, Junin, Calceta, San Isidro, Zapallo, Tosagua, Flavio Alfaro, El Carmen, Boca de Palmito, El Achote, Puerto Cayo, Matiano, Manta, Jaramijó, Boca de Chila, Guachal, Chamanga and Cheve Abajo. Between Cube – Tacusa and Colope, several unstable slopes were observed, which were not affected by the main event, suggesting a recorded intensity with a lower degree of VII. Rockfall in coastal cliffs and damage to the protective wall in the beach area were not observed.

Fig. 25: Fissures in Jaramijó, rockfalls on unstable slopes of cliffs generating accumulated material of less than 150 $m^3$. Intensity ESI = VII. Image courtesy of Global Medical.

Fig. 26: Longitudinal fractures in middle of a paved road in Manta, with openings of 2 to 5 cm, lateral spreading. Coord. UTM: 531735mE 9894912mN.

Concrete roads did not suffer significant damage, in contrast to paved roads that experienced diagonal, tranversal and longitudinal fractures (relative to the road axis) with openings between 2 to 8

cm in sites like Portoviejo, Crucita, Junco - Cerecita, Jaramijó, Manta, San Mateo, San isidro, Mejia Bridge, Junin and Bahia de Caráquez, Cheve, Morascumbo and south of the city of Esmeraldas (UTM coordinates 614.372mE, 10016.254mN). Cracks in natural free-field soil reached widths of 10 cm in areas of floodplains such as Junin. Alluvial terraces and or abandoned flood plain areas experienced cracks of 2 to 4 cm wide, like in Manta and Crucita (Fig. 26). The most notable feature related to this macroseismic intensity, however, has been documented in the Bolvoni site in Portoviejo, where part of the river bank collapsed through rotational and lateral spreading movements causing partial damage to the bridge affecting parked vehicles were affected (Fig. 27). Figure 28 shows ground movements from a single vent in the pavement as recorded by the GEER-ATC team (Nikolaou et al., 2016). Eyewitness accounts indicate that water sprayed out of the ground as high as 1 m immediately following the ground shaking.

Fig. 27: Rotational and lateral ground deformations in the river margin, partial bridge collapse, easily eroded sandy material. Intensity ESI = VII. Bolvoni site, Portoviejo. 560261mE 9882769mN.


Fig. 28: Wall at Portoviejo Velboni site recorded by GEER-ATC (Nikolaou et al., 2016): Slope failure showing two primary slip surfaces and wall rotating, following the slope movement (GPS: 1°3'37.8"S, 80°27'29.3"W).


Fig. 29: Rio Chico: Settlement and rotation of block in foreground and circular global failure in background recorded by GEER-ATC (Nikolaou et al., 2016). (GPS: 0° 58' 36.6" S, 80° 25' 23.7" W).

At the margins of coastal plains of beaches, evidence of lateral spreading was noted through the deformation of cobblestones in the seawall as seen in Bahia de Caraquez, where cracks parallel to the coastline reached openings of 20 cm (coord. UTM: 564.133mE, 9.932.734mN). Damage on bridges by vertical displacement (10 to 15 cm) on the lateral side of the roads were caused by the formation of lateral spreading (Fig. 29). Cracks associated with this phenomenon reached openings of 20 to 25 cm (e.g., floodplain of Calceta, UTM Coord. 593.178mE, 9.906.222mN). Evidence of lateral spreading has been reported in San Mateo, Piedra Larga, Chone, Calceta, Jaramijó, Sesme, Pavon, Mate, Muisne, San Isidro, Portoviejo and Bahia de Caraquez.

Fig. 30: Concentrated sand blow in the center of pavement in the Manta Port parking area (GPS: 0°56'27.6"S, 80°43'29.4"W). (Nikolaou et al., 2016)

Soil liquefaction in alluvial plains such as this observed by GEER-ATC (Nikolaou et al., 2016) at the parking lot of the Manta Port affected networks and induced collapses in Manta where lateral spread was also observed (UTM coord: 605.574mE, 9.925.484mN and 606.894mE, 9.928.506mN). In Chone, subsidence due to soil liquefaction in alluvial terraces has been recorded (UTM Coord. 598.218mE, 9.921.753mN).

Referring to damage sites with lower intensities, such as landslides with less than 50 $m^3$ and minor fractures with openings of 1 cm or less in paved roads, were assigned with and intensity degree of VI, where the evidences in the field are sporadic.

The results of these sampling stations were used to reconstruct a geological map with isoseismals fields of intensities. With the compiled and recorded coseismic data in the field of higher macroseismic intensities, we wer able to produce a map of intensities by applying the definitions and scale of the ESI 2007 scale (Fig. 31).

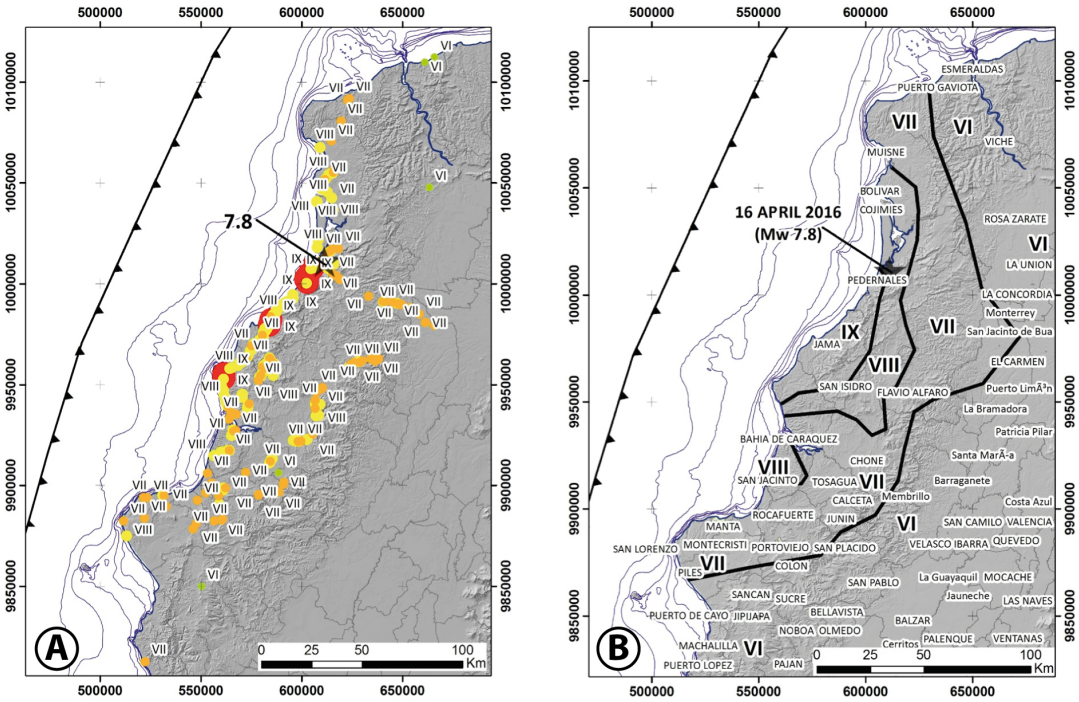


Fig. 31: (a) Seismic intensities of the main $M_w$7.8 earthquake according to the scale ESI-2007; and (b) Zoning of intensity degrees of VI to IX (Chunga et al., 2016).

## 6. EVALUATION OF COLLATERAL TSUNAMI

Worldwide, active continetal rims are capable to trigger massive submarine landlsides or slope failures, which in turn may generate devastating tsunamis (Heezen and Ewing, 1952; Hampton et al., 1996; Driscoll et al., 2000; Ward, 2001; Tappin et al., 2001; 2002; McAdoo and Watts, 2004; Fine et al., 2005; Masson et al., 2006). In such cases, the epicenter does not need to be in the seaside, but can rather be on the (dry) continental zone.

There is not certainty if the April 16$^{th}$ tsunami was triggered by a massive submarine landslide or seafloor coseimic deformation. According to Oceanographic Institute of the Navy, INOCAR, the crest of the tsunami wave arrived to the city of Esmeraldas 6 minutes after the earthquake. This is a very short time for the tsunami travel time from the tsunami landslides scars proposed by Ratzov et al, 2007, and also for the fault plane for the similar 1942 earthquake, as it is demonstrated in Ioualalen et al, 2011. Using both numerical simulation, the tsunami would have arrived more thar 20 minutes from its generation zones. For the case of seismically-induced tsunami, we would need to update the numerical simulation when the focal mechanism is well defined.

Nevertheless, the earthquake of the 16th of April 2016 in Ecuador triggered a tsunami, registered by 32411 and buoys from NOAA located at Panama and Peru basins, respectively. These were registered 2 and 3 hours after the earthquake when the waves passed over their positions. Furthermore, the seismic waves propagated over the seabed, affecting the register at the pressure sensor of these buoys until an hour after the earthquake (Fig. 32). Roughly, we were able to observe that the period of the tsunamis has been about 40 minutes with amplitude close to 1 cm.

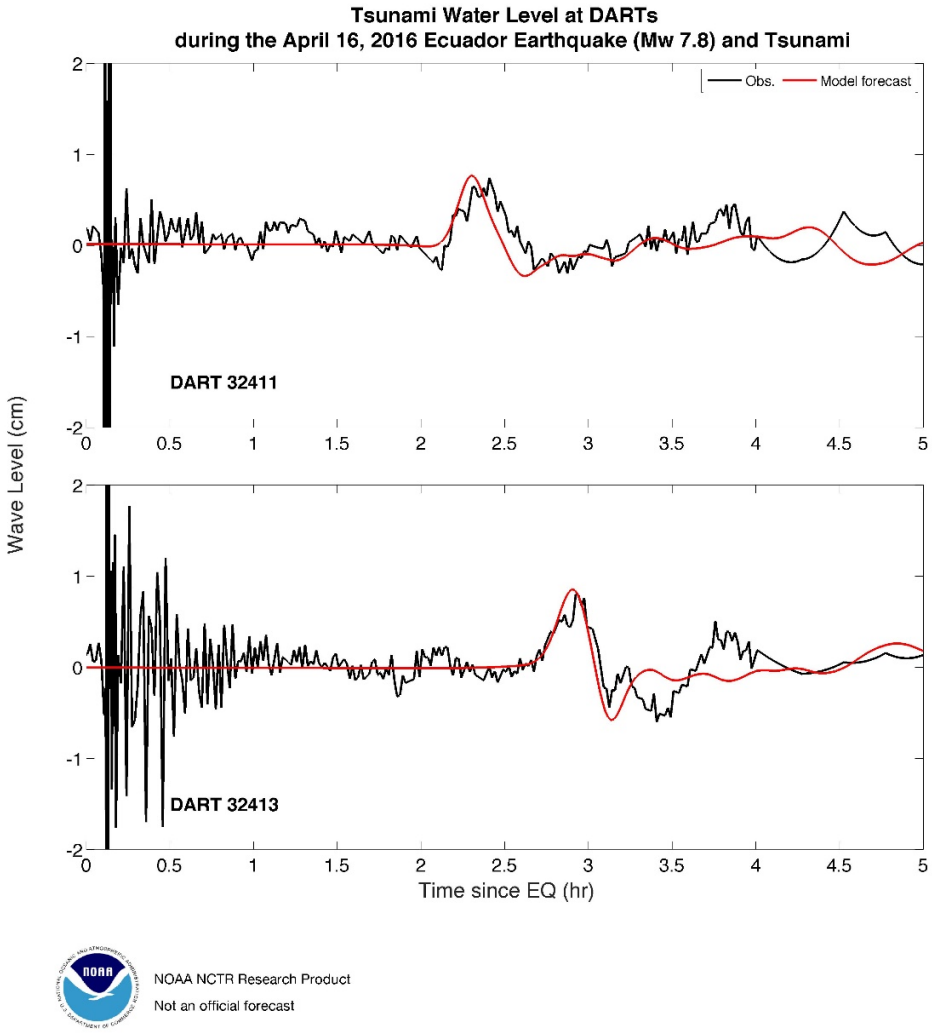


32413 DART

Fig. 32: Register of oceanic propagation of the tsunami at DART Buoy position. SOURCE: NOAA

Locally, the tsunami was registered by the INOCAR-DART buoy, which is close to the epicenter, immediately after the earthquake. It has been difficult to differentiate the tsunami signal from the noise produced by the earthquake, however it is notable that the perturbation exist after the earthquake time, changing the initial conditions in the calm water level (Fig. 33).

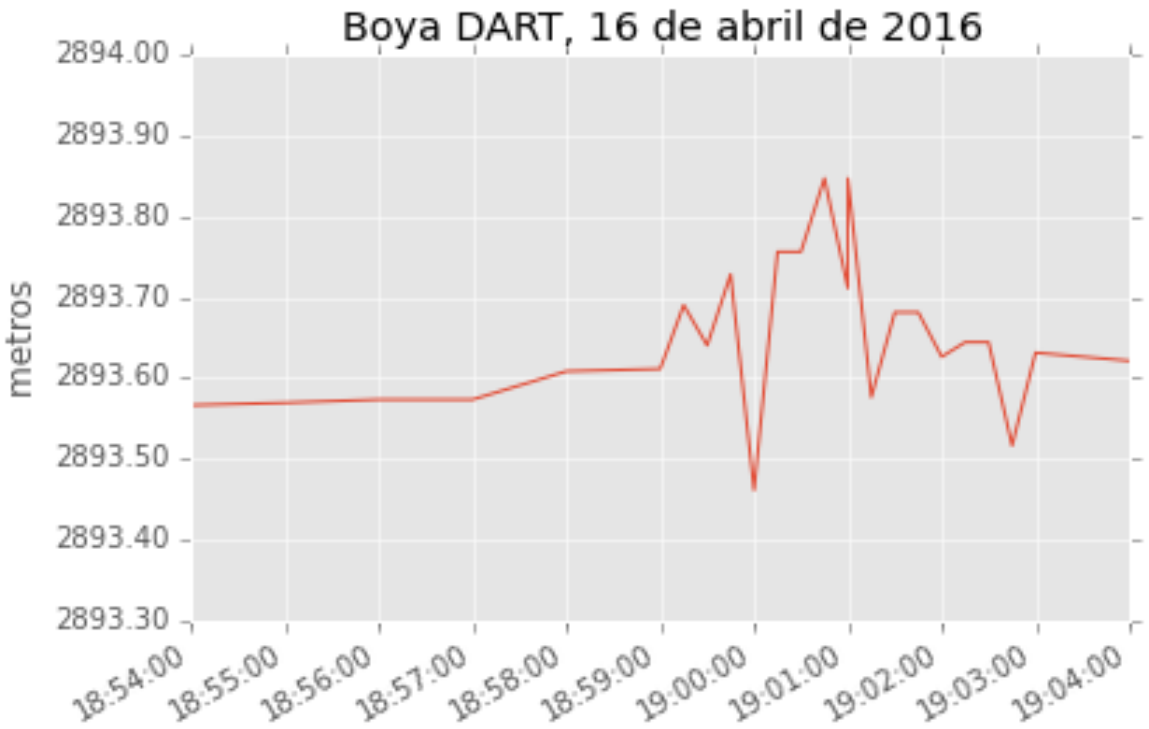


Figure 33 Tsunami sea level perturbations. Source: INOCAR.

INOCAR issued a Tsunami Warning over the entire Ecuadorian coast based on the data from the INOCAR-DATA buoy with remained in effect 4 hours after the event, considering the potential threat to the shores of the nearby Galapagos Islands.

Several people at the coastal communities reported remarkable changes in the seawater level and also strong rift currents, although the amplitude of the tsunami did not reach any high water level. Fortunately for these coastal communities, the tsunami impact occurred at low tide. This important fact appears to be the reason that no inundation occurred and considerable physical effects at the coastalines have been absent. However, this case could have been catastrophic under different tide conditions. It should be noted that some of the authorities were not alerted for a tsunami hazard due to the false perception that a tsunami would not be possible because the epicenter in the continental and not on the marine side.

The Esmeraldas Port registered the arrival of tsunami with the receiding of the water, which started at 19:00. From 19:06 to 19:09, the tide gauge registered the arrival of the tsunami crest which meant a rate of change in water level of ~50 cm/min. (Fig. 34)

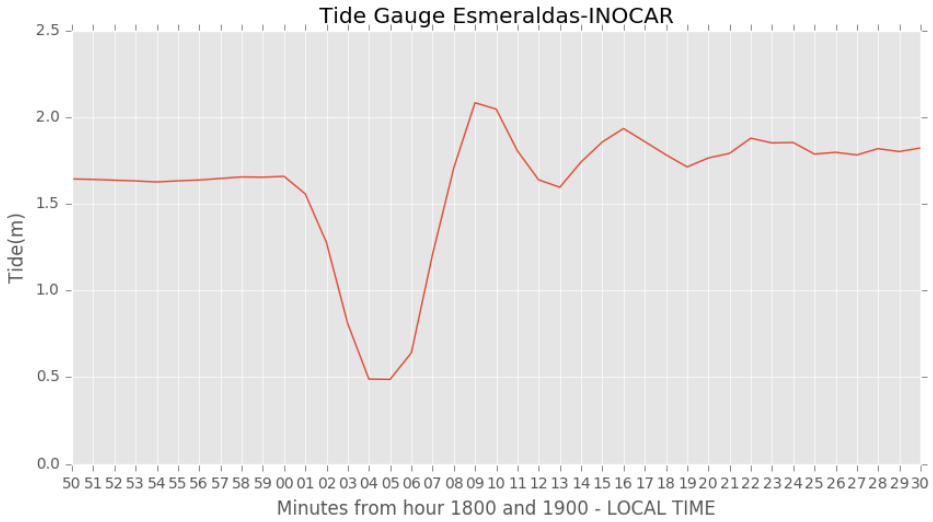


Fig. 34: Mareogram from Esmeraldas Tide Gauge. Note that tsunami crest wave arrived 6 minutes after the event. Source: INOCAR

Even with the arrival tsunami at low tide, the Esmeraldas Port was exposed to strong residual currents. Some small boats and buoys were moved from these anchorage sites due the strong currents (Fig. 35).


Fig. 35: Fishing Port Esmeraldas. At the time of tsunami arrival, a small boat and buoys set were moved from their anchorage. Source: ECU911

## 7. ECONOMIC DAMAGE

Natural disasters become an obstacle to economic development, particularly in small, less developed countries (Ferris and Petz, 2012; Kahn, 2005). A recent report by the United Nations (UNISDR, 2016) concludes that natural disasters in the Latin-American region have increased as have the losses in human life and economy that can reach a significant portion of the nation's Gross Domestic Product (GDP). In comparison to countries with social expenditures, it could reach between 30 up to 50% of social expenditures (UNISDR/Corporación OSSO, 2016).

According to the Ecuadorian government, the estimated total loss was a little over 3.3 billionUS$ being equivalent to 3.3% of the Ecuadorian GDP (SNGR, 2016; El Universo, 2016). A total of 29,672 properties, including family houses were affected and so far at least 5,000 have been demolished (El Universo, 2016). Insurance companies paid some 134 US$ million in disaster coverage (El Universo, 2016) three months after the earthquake. Regarding infrastructure, such as the Ecuadorean Pacific Highway, 70 km have been affected in the Province of Manabi alone and its reconstruction cost is estimated at 35 million US$ (El Universo, 2016). In addition to losses in infrastructure and properties, over 28,000 jobs were lost and about 300 million US$ in trade and businesses. Over 7,000 businesseds were directly affected, some of which may have to declare bankruptcy. From the people affected, 97% did not have savings and 23% did not have property rights or any way to prove ownership of their homes (El Universo, 2016).

The recent earthquake has been one of the most devastating natural disasters in recent decades in Ecuador as shown on Table 1 that compares it to other historic earthquakes. The 2016 event claimed the second largest ever loss of life, but the highest amount of injured, while it ranks 5$^{th}$ in home losses. However, this earthquake has been the most devastating in terms of economic damage. The cost estimated do not include cost of recovery teams, firefighters and volunteers, who have been successful and efficient not only in terms of efforts and time, but also the impact these people have had in the local population (El Universo, 2016).

Table 1. Comparison of historic earthquake effects. Source: EM-DATA, CRED/IRSS 2016

| Year | Disasters | Killed | Injured | Affected | Homeless | Total affected | Total dam x million |
|---|---|---|---|---|---|---|---|
| 1970 | 1 | 29 | 120 | 60000 | 27992 | 88112 | 4,00 |
| 1976 | 2 | 20 | - | - | 20000 | 20000 | 4,00 |
| 1980 | 1 | 8 | 40 | - | - | 40 | - |
| 1987 | 2 | 5002 | 6 | 4500 | 15000 | 19506 | 1500,00 |
| 1990 | 1 | 4 | 10 | 6500 | - | 6510 | - |
| 1995 | 2 | 3 | 90 | 200 | 600 | 890 | - |
| 1996 | 1 | 27 | 180 | 15000 | 15525 | 30705 | 7,00 |
| 1998 | 1 | 3 | 40 | 1250 | 750 | 2040 | - |
| 2014 | 1 | 3 | 18 | - | - | 18 | - |
| 2016 | 1 | 671 | 4859 | 70000 | 11400 | 81400 | 3344,00 |

The second decade of this millennium has been particularly active in terms of earthquakes and tsunamis along the Pacific "Ring of Fire." The mega-earthquake and associated tsunami of Chile on February 27th, 2010 claimed 525 lifes and generated an economic loss of 24 billion US$, representing about 12% of country's GDP (Insurance Information Institute, 2016; Biblioteca del Congreso Nacional de Chile, 2010). About a year later, on March 11th, 2011, Japan was hit by a mega-earthquake and tsunami with death toll of 15,854 people and an economic loss reaching 309 billion US$ (6% of Japan's GDP), destroying about 650 businesses (Insurance Information Institute, 2016). New Zealand was hit by a sequence of earthquakes with main events on February 21st and June 13th 2011, leaving economic losses of about 40 billion US$, representing 28% of the country's GDP, in addition to killing 185 persons (Insurance Information Institute. 2016). Based on the International Disaster Database EM-DAT, Figure 36 demonstrates the increase in earthquake-induced economic losses around the Pacific Ocean´s countries since 1951 (CRED, 2016).

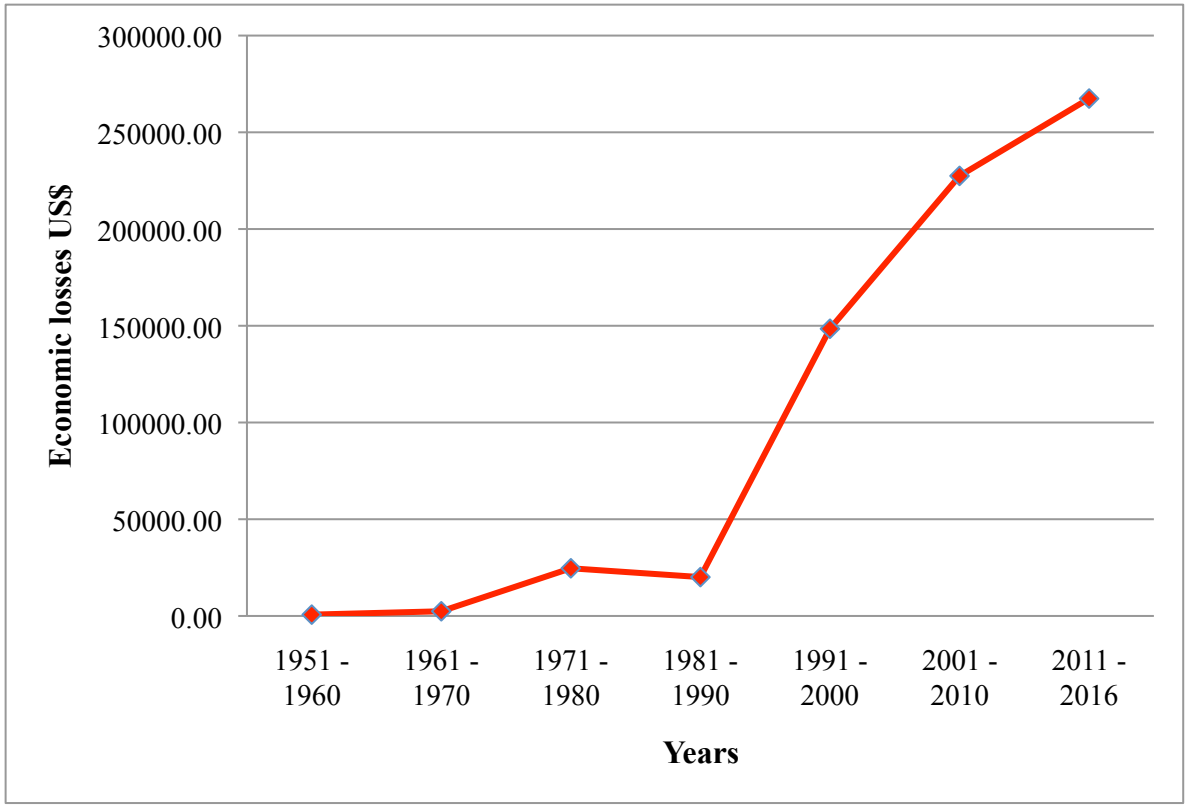


Fig. 36: Earthquake-induced economic losses around the Pacific Ocean´s countries since 1951 (CRED, 2016).

Table 2 presents economic losses in US$ in countries in the Pacific Ring of Fire as function of the decade since 1951. China, Chile and Japan are the most affected countries since 1951 in economic damages (Insurance Information Institute. 2016). However, China had several earthquakes in the last few decades, but only one caused an enormous economic impact on its GDP. The 2008 earthquake induced economic losses of 4% of China's GDP (Insurance Information Institute. 2016). Meanwhile,

Chile and Japan have had at least one major earthquake and/or tsunami each decade since 1961. New Zealand's economy has also been critically affected by repeateative earthquakes with the 2011 sequence affecting international trade totaling 28% of its GDP in economic losses (Insurance Information Institute. 2016).

Ecuador, as well as Mexico have been hit by earthquakes and tsunamis almost once in each decade and the destruction has been severe with economic losses exceeding 4.8 billion US$ since 1951 (Insurance Information Institute. 2016).

Table 2: Economic effects per decade by natural disasters of some selected countries. Source: EM-DATA, CRED/IRSS 2016; INSURANCE INFORMATION INSTITUTE 2016

| COUNTRY | 1951 - 1960 | 1961 - 1970 | 1971 - 1980 | 1981 - 1990 | 1991 - 2000 | 2001 - 2010 | 2011 - 2016 | TOTAL COUNTRY |
|---|---|---|---|---|---|---|---|---|
| Chile | 550,0 | 360,4 | 236,4 | 1501,0 | 49,7 | 30105,0 | 24000,0 | 56802,5 |
| China | | | 22900,0 | | | 137500,0 | 5025,0 | 165425,0 |
| Colombia | 0 | 1,0 | 28,0 | 410,9 | 1859,8 | 10,0 | 4,0 | 2313,7 |
| Costa Rica | 0 | 0,0 | 0,2 | 20,5 | 100,0 | 200,0 | 45,0 | 365,7 |
| Ecuador | 0 | 4,0 | 4,0 | 1500,0 | 7,0 | 0,0 | 3344,0 | 4859,0 |
| El Salvador | 0 | 35,0 | 0 | 1500,0 | 0 | 1848,5 | 0 | 3383,5 |
| Honduras | 0 | 0 | 0 | 0 | 0 | 100,0 | 0 | 100,00 |
| Japan | 140,0 | 931,0 | 865,0 | 459,0 | 102028,4 | 43534,0 | 210000,0 | 357957,4 |
| Mexico | 0 | 3,0 | 30,0 | 4104,0 | 412,7 | 1266,3 | 320,0 | 6136,0 |
| New Zealand | 0 | 0 | 0 | 210 | 0 | 10000,0 | 24000,0 | 34210,0 |
| Peru | 0 | 552,1 | 30,0 | 23,0 | 0,0 | 900,1 | 0,0 | 1505,2 |
| United States | 0 | 540,0 | 550,0 | 10360,0 | 44000,0 | 2000,0 | 700,0 | 58150,0 |
| TOTAL | 690,00 | 2426,5 | 24643,6 | 20088,4 | 148457,5 | 227463,9 | 267438,0 | 691207,9 |

The 2016 earthquake in Ecuador had the most severe economic effect in this country as demonstrated in Table 2, in addition to being the second deadliest event since 1949 (Secretaria Nacional de Riesgo, 2016). During the recovery process, Ecuador received loans from multilateral organizations such as Inter-American Development Bank (BID), International Monetary Fund (IMF), World Bank (WB), and Latin-American Development Bank among others, totaling about 914 million $US. Ecuador received also a little over 180 million $ US from the International Cooperation and Disaster relief and from several governments, as well as international organizations including the UNO with 73 million $US 2 million $US from China, 100 million $US from Spain, 5.5 million $US from the United States of America and some 1,1 million $US from the European Union (El Universo, 2016).

All these funds and loans will cover approximately 37% of the total damage and reconstruction costs. Another third of the total cost will be covered by the increase in taxes such Added Value Tax, which has increased from 12% to up to 14% (Martínez and EL Comercio-DATA, 2016). Due to the absent international monetary reserves, weak financial institutions and low prices of commodities such as oil and minerals, the recovery process will take some time (World Bank, 2016). These fragile economic

predictions are supported by the reduced growth estimates of Ecuador which, for 2016, was -4.5% as reported by the IMF. Under these conditions, the reconstruction total costs may reach between 15 to up to 30 billion US$, based on estimates from economic losses from Chile and Haiti earthquakes (Biblioteca del Congreso Nacional de Chile, 2010; Cavallo et al., 2010; UNISDR/Corporación OSSO, 2016).

The April 16th, 2016 earthquake in Pacific coast of Ecuador took place in moments of a contraction of Ecuadorean economy, due to external effects such as oil prices plunge in 2015. According to IMF, the economic impact of 3.344 billion US$ GDP reduced its growth in 4.5% (0.5% of the 2.25% of the contraction expected), so it will take years to come back to previous economic conditions. From the economic point of view, a trust fund or other type of financial instrument would reduce such economical impact in terms of speeding up nation's recovery. Nonetheless, an overall conclusion based on the observations and estimated effects of this natural disaster, is that a radical changes in several directions are necessary to rebuild the country targeting effective resillence goals: (1) an improvement in the national seismic monitoring means with automated and verified information to be rapidly provided to scientists and stakeholders after an earthquake with verified epicenter location and magnitude estimate; (2) advanced planning for the response and decision-making chain; (3) implementation of a national research network for early warning in seismic hazards and a national earthquake center; (4) improvement of the national building code to include seismic risk assessment and management; (5) implementation of inspection quality control in the implementation of building normatives; (6) development of a clear awareness, preparation, and response plan for the public, including shake-out exercises (7) development and implementation of a dedicated national emergency unit with all necessary disciplines involved; (8) creation of long-plan resilience goals for infrastructure networks; and (9) evaluation of multi-hazard exposure of the country to other natural phenomena.

Finally, about the tsunami hazard in particular, more research is needed to clarify if the tsunami was triggered by a landslide or by the earthquake itself. This research should include bathymetric surveys and multitemporal analysis to identify the scars or the seafloor deformation. A better estimation of the focal mechanism of the main event is important in order to simulate a synthetic tsunami, to mimic the mareograms obtained at Esmeraldas Port. Moreover, the strong currents generated by the tsunami arrival must be considered by the Maritime Authority for the development of Contingency Plans, since these occurred even when the tsunami not caused an inundation in the coastal basin.

**Acknowledgements**

The authors acknowledge the collaboration and exchange of information with the US reconnaissance team of the Geotechnical Extreme Events Reconnaisance (GEER) Association, funded by the National Science Foundation (NSF), and the Applied Technology Council (ATC) are gratefully acknowledged. Fernando Mato also acknowledges support from the Prometeo Project of the National Secretariat of Higher Education, Science, Technology and Innovation (SENESCYT), Ecuador.

## REFERENCES


Anbarci, N., Escaleras, M. and Register, C.A., 2005. Earthquake fatalities: the interaction of nature and political economy. Journal of Public Economics, 89(9): 1907-1933.

Baldock, J.W., 1982. Geology of Ecuador: explanatory bulletin of the national geological map of the Republic of Ecuador; 1: 1,000,000 scale. Ministerio de Recursos Naturales y Energéticos, Dirección General de Geología y Minas, Quito, Ecuador: 54pp

Bardet, J.P., Synolakis, C.E., Davies, H.L., Imamura, F. and Okal, E.A., 2003. Landslide tsunamis: Recent findings and research directions. Birkhäuser Basel: 1793-1809.

Beck, S.L. and Ruff, L.J., 1984: The rupture process of the great 1979 Colombia earthquake: evidence for the asperity model. J.Geophys. Res., 89: 9281–9291

Bender, B. (1983): Maximum likelihood estimation of b values for magnitude grouped data, Bull. Seismol. Soc. Am., 73: 831-851

Berninghausen, W.H., 1962. Tsunamis reported from the west coast of South America 1562-1960. Bull. of the Seismological Soc. of America, 52 (4): 915-921.

Biblioteca del Congreso Nacional de Chile. 2010. Efectos Económicos del Terremoto en Chile, por sectores y enel empleo: Una evaluación preliminar. BCN Informe, Santiago, Chile: 7pp.

Bristow, C.R. and Hoffstetter, R., 1977. Lexique Stratigraphique International; Ecuador. Second edition. Paris: Centre National de la Recherche Scientifique: 412p

Bryant, E., 2014. Tsunami: the underrated hazard. Springer: 222pp

Butler, R., Stewart, G.S. and Kanamori, H., 1979. The July 27, 1976 Tangshan, China earthquake—a complex sequence of intraplate events. Bulletin of the Seismological Society of America, 69(1): 207-220.

Cavallo, E.A., Powell A. and Becerra, O. 2010: Estimating the Direct Economic Damage of the Earthquake in Haiti.IDB Working Paper Series No.IDB-WP-163. The Inter American Development Bank; Department of Research and Chief Economist. Washington DC. 16 pp.

Chen, Y. ed., 1988. The great Tangshan earthquake of 1976: an anatomy of disaster. Pergamon: 162pp

Chunga, K., Besenzon, D., Mulas, M., Loayza, G. and Pindo JC., 2016: Areal distribution of Ground effects induced by the 2016 Mw 7.8 Pedernales earthquake (Ecuador). 88° Congresso della Societa' Geologica Italiana. S1. Earthquakes and Active Tectonics: a multidisciplinary approach. Napoli, 7/9 sept.

Chunga, K. and Toulkeridis, T. (2014). First evidence of paleo-tsunami deposits of a major historic event in Ecuador. J. Tsunami Soc. Int, 33: 55-69.

Collot, J.-Y., Michaud, F., Alvarado, A., Marcaillou, B., Sosson, M., Ratzov, G., Migeon, S., Calahorrano, A. and Pazmino, A., 2010. Vision general de la morfologa submarina del margen convergente de Ecuador-Sur de Colombia: implicaciones sobre la transferencia de masa y la edad de la subduccion de la Cordillera de Carnegie, in Sintesis de los Resultados de Investigacion Geologica y Geofisica Sobre el Margen Ecuatoriano, la Costa, la Cordillera Submarina de Carnegie, y de la Plataforma Volcanica de Galapagos, eds Collot, J.-Y., Sallares, V. & Pazmio, A., Publicacion CNDM-INOCAR-IRD, PSE001-09, Guayaquil, Ecuador: 47–74.





Collot, J.-Y., Michaud, F., Legonidec, Y., Calahorrano, A., Sage, F., Alvarado, A. & el personal

cientifico y tecnico del INOCAR, 2005. Mapas del margen continental centro y sur de Ecuador: Bathymetria, relieve, refllectividad acustica e interpretacion geologica, Publicacion IOA - CVM- 04 - POST.

Collot, J.Y., Marcaillou, B., Sage, F., Michaud, F., Agudelo, W., Charvis, P., Graindorge, D., Gutscher, M.A. and Spence, G., 2004. Are rupture zone limits of great subduction earthquakes controlled by upper plate structures? Evidence from multichannel seismic reflection data acquired across the northern Ecuador–southwest Colombia margin. Journal of Geophysical Research: Solid Earth, 109(B11).

CRED (Centre for Research on the Epidemiology of Disasters) 2016: http://www.cred.be/node/1516

Driscoll, N.W., Weissel, J.K. and Goff, J.A., 2000. Potential for large-scale submarine slope failure and tsunami generation along the US mid-Atlantic coast. Geology, 28(5), pp.407-410.

Egbue, O. and Kellogg, J., 2010: Pleistocene to Present North Andean "escape". Tectonophysics 489: 248-257.

El Telegrafo, 2016: http://www.eltelegrafo.com.ec/noticias/ecuador/3/manana-se-daran-a-conocer-cifras-oficiales-del-costo-del-terremoto

El Universo, 2016: http://www.eluniverso.com/noticias/2016/04/25/nota/5544318/multilaterales-paises-ong-envian-recursos-exterior

Feininger, T. 1980. La geología histórica del Cretácico y el Paleógeno de la Costa Ecuatoriana, Politécnica, Monograf. Geología, V, 2: 7-48.

Ferris E. and Petz D. 2012. The year shock the rich: A review of natural disasters in 2011. Project on Internal Displacement, The Brookings Institution-The London School of Economics. Washington DC. 142 pp.

Fine I.V, Rabinovich A.B, Bornhold B.D, Thomson R.E, Kulikov E.A 2005 The Grand Banks landslide-generated tsunami of November 18, 1929: preliminary analysis and numerical modelling. Mar. Geol. 215, 45–57

Gang, Q., 1989: The Great China Earthquake. Beijing: Foreign Languages Press. 354pp

GEER-ATC Report (GEER-049), Nikolaou, S., Vera-Grunauer, X., Gilsanz, R. eds., "2016 Ecuador GEER-ATC Report version 1". Published in geerassociation.org: http://www.geerassociation.org/component/geer_reports/?view=geerreports&id=77&layout=default

Ghobarah, A., Saatcioglu, M. and Nistor, I., 2006. The impact of the 26 December 2004 earthquake and tsunami on structures and infrastructure. Engineering structures, 28(2): 312-326.

Gupta, H.K., Rao, N.P., Rastogi, B.K. and Sarkar, D., 2001. The deadliest intraplate earthquake. Science, 291(5511): 2101-2102.

Gusiakov, V.K., 2005: Tsunami generation potential of different tsunamigenic regions in the Pacific. Marine Geology, 215, 1-2: 3-9.

Gutenberg, B., 1939. Tsunamis and earthquakes. Bulletin of the Seismological Society of America, 29(4): 517-526.

Gutscher, M.A., Malavieille, J.S.L. and Collot, J.-Y., 1999: Tectonic segmentation of the North Andean margin: impact of the Carnegie ridge collision. Earth Planet. Sci. Lett. 168: 255–270.



Hampton M.A, Lee H.J, Locat J 1996 Submarine landslides. Rev. Geophys. 34: 33–59.

Harpp, K. S. and White, W. M., 2001: Tracing a mantle plume: Isotopic and trace element variations of Galápagos seamounts. Geochemistry, Geophysics, Geosystems, 2(6).

Harpp, K. S., Fornari, D. J., Geist, D. J. and Kurz, M. D., 2003: Genovesa Submarine Ridge: A manifestation of plume-ridge interaction in the northern Galápagos Islands. Geochemistry, Geophysics, Geosystems, 4(9).

Heezen B.C, Ewing M 1952 Turbidity currents and submarine slumps, and the 1929 Grand Banks Earthquake. Am. J. Sci. 250: 775–793.

Holden, J. C. and Dietz, R. S. (1972). Galapagos gore, NazCoPac triple junction and Carnegie/Cocos ridges. Nature, 235: 266-269.

Holzer, T.L. and Savage, J.C., 2013. Global earthquake fatalities and population. Earthquake Spectra, 29(1): 155-175.

Hou, J.J., Han, M.K., Chai, B.L. and Han, H.Y., 1998. Geomorphological observations of active faults in the epicentral region of the Huaxian large earthquake in 1556 in Shaanxi Province, China. Journal of structural geology, 20(5): 549-557.

Insurance Information Institute, 2016, Earthquakes and Tsunamis, Insurance Information Institute Insurance topics, from: http://www.iii.org/fact-statistic/earthquakes-and-tsunamis

International Monetary Fund. 2016. Ecuador and the IMF. Country Info August 8 2016. International Monetary Fund, Washington DC: https://www.imf.org/external/country/ECU/index.htm

IGEPN (Instituto Geofísico Escuela Politécnica Nacional), 2016a: Informe Sísmico Especial Nº 22, 2016. www.igepn.edu.ec/servicios/noticias/1341-informe-sismico-especial-n-22-2016

IGEPN (Instituto Geofísico Escuela Politécnica Nacional), 2016b: Earthquake Overview. www.igepn.edu.ec

Ioualalen, M., Ratzov, G., Collot, J.Y. and Sanclemente, E., 2011. The tsunami signature on a submerged promontory: the case study of the Atacames Promontory, Ecuador. Geophysical Journal International, 184(2): 680-688.

Kahn, M.E., 2005. The death toll from natural disasters: the role of income, geography, and institutions. Review of economics and statistics, 87(2): 271-284.

Kanamori, H. and McNally, K.C., 1982. Variable rupture mode of the subduction zone along the Ecuador-Colombia coast. Bulletin of the Seismological Society of America, 72(4): 1241-1253.

Kelleher, J.A., 1972: Ruptures zones of large South American earthquakes and some predictions. Journal of Geophysical Research, 77, 11: 2087-2103.

Kellogg, J.N. and Vega, V., 1995: Tectonic development of Panama, Costa Rica and the Colombian Andes: Constraints from Global Positioning System geodetic studies and gravity. Geol. Soc. Am. Special Paper 295: 75–90.

Lebrat, M., Megard, F., Dupuy, C and Dostal, J., 1987: Geochemistry and tectonic setting of pre-collision Cretaceous and Paleogene volcanic rocks of Ecuador. Bulletin of the geological society of America, 99: 569-578.

Marano, K.D., Wald, D.J. and Allen, T.I., 2010. Global earthquake casualties due to secondary effects: a quantitative analysis for improving rapid loss analyses. Natural hazards, 52(2): 319-328.

Martínez, S. and El Comercio DATA. 2016: Conozca 208 bienes y servicios que pagarán 14% de IVA en Ecuador. Sección El Comercio-DATA, Compañía Anómima El Comercio, Quito, Ecuador. http://www.elcomercio.com/datos/servicios-productos-aumento-iva-ecuador.html

Masson, D.G., Harbitz, C.B., Wynn, R.B., Pedersen, G. and Løvholt, F., 2006: Submarine landslides: processes, triggers and hazard prediction. Philosophical Transactions of the Royal Society of London A: Mathematical, Physical and Engineering Sciences, 364(1845): 2009-2039.

McAdoo, B.G. and Watts, P., 2004: Tsunami hazard from submarine landslides on the Oregon continental slope. Marine Geology, 203(3): 235-245.

McCaffrey, R., 2008. Global frequency of magnitude 9 earthquakes. Geology, 36(3): 263-266.

McGuire, R.K., 1995. Probabilistic seismic hazard analysis and design earthquakes: closing the loop. Bulletin of the Seismological Society of America, 85(5): 1275-1284.

Michetti A.M., Esposito E., Guerrieri L., Porfido S., Serva L., Tatevossian R., Vittori E., Audemard F., Azuma T., Clague J., Comerci V., Gürpinar A., McCalpin J., Mohammadioun B., Mörner N.A., Ota Y. and Rogozhin E., 2007:. Intensity Scale ESI 2007. La Scala di Intensità ESI 2007, ed. L. Guerrieri e E. Vittori (Memorie Descrittive della Carta Geologica d'Italia, vol.74, Servizio Geologico d'Italia – Dipartimento Difesa del Suolo, APAT), Roma, http://www.apat.gov.it/site/it-IT/Progetti/-INQUA_Scale/.

Papanikolaou, I.D., Foumelis, M., Parcharidis, I., Lekkas, E.L. and Fountoulis, I.G., 2010: Deformation pattern of the 6 and 7 April 2009, MW= 6.3 and MW= 5.6 earthquakes in L'Aquila (Central Italy) revealed by ground and space based observations. Nat. Hazards Earth Syst. Sci, 10(1): 73-87.

Pararas-Carayannis, G. 1980: The Earthquake and Tsunami of December 12, 1979, in Colombia. Intern. Tsunami Information Center Report, Abstracted article in Tsunami Newsletter, Vol. XIII, No. 1.

Pararas-Carayannis, G., 1967: A study of the source mechanism of the Alaska earthquake and tsunami of March 27, 1964: Part I, Water waves. Pacific Science, 21: 301-310.

Pararas-Carayannis, G., 2006: The potential of tsunami generation along the Makran Subduction Zone in the northern Arabian Sea: Case study: The earthquake and tsunami of November 28, 1945. Science of Tsunami Hazards, 24(5): 358-384.

Pararas-Carayannis, G., 2010: The earthquake and tsunami of 27 February 2010 in Chile–Evaluation of source mechanism and of near and far-field tsunami effects. Science of Tsunami Hazards, 29, 2: 96-126.

Pararas-Carayannis, G., 2012: Potential of tsunami generation along the Colombia/Ecuador subduction margin and the Dolores-Guayaquil Mega-Thrust. Science of Tsunami Hazards, 31, 3: 209-230.

Pararas-Carayannis, G., 2014. The Great Tohoku-Oki earthquake and tsunami of March 11, 2011 in Japan: A critical review and evaluation of the tsunami source mechanism. Pure and applied geophysics, 171(12): 3257-3278.

Parra, H; Benito, B, Gaspar-Escribano, J. (2016). Seismic Hazard Assessment in Continental Ecuador. Bull Earthquake Eng., 1-31. DOI 10.1007/s10518-016-9906-7

Pilger, R. H., 1983. Kinematics of the South American subduction zone from global plate reconstructions. Geodynamics of the eastern Pacific region, Caribbean and Scotia arcs: 113-125.

Pontoise, B. and Monfret, T. (2004). Shallow seismogenic zone detected from an offshore‐onshore temporary seismic network in the Esmeraldas area (northern Ecuador). Geochemistry, Geophysics, Geosystems, 5(2).

Raschky, P.A. 2008. Institutions and the losses from natural disasters. Natural Hazards and Earth System Science 8: 627-634.

Ratzov, G., Collot, J. Y., Sosson, M. and Migeon, S. (2010). Mass-transport deposits in the northern Ecuador subduction trench: Result of frontal erosion over multiple seismic cycles. Earth and Planetary Science Letters, 296(1): 89-102.

Ratzov, G., Sosson, M., Collot, J. Y., Migeon, S., Michaud, F., Lopez, E. and Le Gonidec, Y. (2007). Submarine landslides along the North Ecuador–South Colombia convergent margin: possible tectonic control. In Submarine Mass Movements and Their Consequences. Springer Netherlands: 47-55

Reyes, P & Michaud, F, 2012 "Mapa Geológico de la Margen Costera Ecuatoriana", 1:500.000. Petroecuador – EP – IRD (Eds). Quito Ecuador.

Reynaud, C., Jaillard, É., Lapierre, H., Mamberti, M. and Mascle, G. H. (1999). Oceanic plateau and island arcs of southwestern Ecuador: their place in the geodynamic evolution of northwestern South America. Tectonophysics, 307(3): 235-254.

Rodriguez, F., DHowitt, M.C., Toulkeridis, T., Salazar, R., Romero, G.E.R., Moya, V.A.R. and Padilla, O., 2016. The economic evaluation and significance of an early relocation versus complete destruction by a potential tsunami of a coastal city in Ecuador. Journal of Tsunami Society International, 35(1). 18-35

Rudolph E. and Szirtes S., 1911: Das kolumbianische Erdbeben am 31 Januar 1906, Gerlands Beitr. z. Geophysik , 2: 132- 275.

Ruff, L.J., and Kanamori, H., 1980, Seismicity and the subduction process: Physics of the Earth and Planetary Interiors, v. 23: 240–252, doi: 10.1016/0031–9201(80)90117-X.

Sato, H., Fehler, M.C. and Maeda, T., 2012. Seismic wave propagation and scattering in the heterogeneous earth, Berlin: Springer. 496pp

Secretaria Nacional de Gestión de Riesgos-SNGR. 2016. Informe de Siatuación No. 71. Equipo Técnico de la Secretaría de Gestión de Riesgos, SNGR. 15 pp. http://www.gestionderiesgos.gob.ec/wp-content/uploads/downloads/2016/05/INFORME-n71-SISMO-78-20302.pdf

Senplades. 2016. Evaluación de los Costos de Reconstrucción Sismo en Ecuador, abril 2016.Secretaría Nacional de Planificación y Desarrollo - Senplades, Quito, Ecuador. 20 pp.

Shepperd, G.L. and Moberly, R., 1981: Coastal structure of the continental margin, northwest Peru and southwest Ecuador. Geological Society of America Memoirs, 154: 351-392,

Shome, N., Cornell, C.A., Bazzurro, P. and Carballo, J.E., 1998. Earthquakes, records, and nonlinear responses. Earthquake Spectra, 14(3): 469-500.

Sieh K 2005 Aceh-Andaman earthquake: What happened and what's next?. Nature. 434: 573–574

Stainforth, R.M. 1948. Applied micropaleontology in Coastal Ecuador, Jour. Paleontology, 22, 142-146.

Swenson, J.L. and Beck, S.L., 1996: Historical 1942 Ecuador and 1942 Peru subduction earthquakes, and earthquake cycles along Colombia–Ecuador and Peru subduction segments. Pure Appl. Geophys.146 (1): 67–101.

Synolakis, C.E., Bardet, J.P., Borrero, J.C., Davies, H.L., Okal, E.A., Silver, E.A., Sweet, S. and Tappin, D.R., 2002, April. The slump origin of the 1998 Papua New Guinea tsunami. In Proceedings of the Royal Society of London A: Mathematical, Physical and Engineering Sciences, Vol. 458, No. 2020: 763-789.

Tappin, D.R., Watts, P., McMurtry, G.M., Lafoy, Y., Matsumoto, T., 2001. The Sissano Papua New Guinea tsunami of July 1998 - ofshore evidence on the source mechanism. Mar. Geol. 175, 1-23; Nature 379(18): 246-249.

Tappin, D.R., Watts, P., McMurtry, G.M., Lafoy, Y., Matsumoto, T., 2002. Prediction of slump generated tsunamis: The July 17, 1998 Papua New Guinea event. Sci. Tsunami Hazards 20: 222-238.

The World Bank. 2016. Ecuador Overview. World Bank – Ecuador home. Washington DC: http://www.worldbank.org/en/country/ecuador/overview

Tierra, A., Toulkeridis, T., Sani, J., Padilla Almeida, O. and Parra, H., 2017: Evaluation of horizontal and vertical positions obtained from an unmanned aircraft vehicle applied to large scale cartography of Infrastructure loss due to the Earthquake of April 2016 in Ecuador. Journal of Disaster Research, in press

Tinti, S., Armigliato, A., Pagnoni, G. and Zaniboni, F., 2005. Scenarios of giant tsunamis of tectonic origin in the Mediterranean. ISET Journal of Earthquake Technology, 42(4): 171-188.

Toulkeridis et al., 2017b; Real-Time Radioactive Precursor of the April 16, 2016 Mw 7.8 Earthquake in Ecuador. Submitted

Toulkeridis, T., Parra, H., Mato, F., Cruz D´Howitt, M., Sandoval, W., Padilla Almeida, O., Rentería, W., Rodríguez Espinosa, F., Salazar martinez, R., Cueva Girón, J., Taipe Quispe, A. and Bernaza Quiñonez, L., 2017a: Contrasting results of potential tsunami hazards in Muisne, central coast of Ecuador. J. Tsunami Soc. Int, 36: 13-40.

Toulkeridis, 2011: Volcanic Galápagos Volcánico. Ediecuatorial, Quito, Ecuador: 364 pp

Tschopp, H.J. 1953. Oil exploration in the Oriente of Ecuador. Bull.AAPG, 37: 2303-2347.

UNISDR, Corporación OSSO, 2016: Impacto de los desastres en América latina y el Caribe 1990-2013: Tendencias y estadísticas para 22 países. Oficina de las Naciones Unidas para la Reducción del Riesgo de Desastres-ININSDR, Agencia Española de Cooperación Internacional para el Desarrollo-aecid, Corporación OSSO: 70 pp.

USGS (United States Geological Service), 2016a: Historic Earthquakes, 1906 January 31st. (http://earthquake.usgs.gov/earthquakes/world/events/1906_01_31.php)

USGS (United States Geological Service), 2016b: M7.8 - 29km SSE of Muisne, Ecuador.http://earthquake.usgs.gov/earthquakes/eventpage/us20005j32#general

USGS (United States Geological Service), 2016c: Earthquake Glossary - aftershocks.https://earthquake.usgs.gov/learn/glossary/?term=aftershocks

USGS (United States Geological Service), 2016d: Earthquake Catalog Search.https://earthquake.usgs.gov/earthquakes/search/

Ward S.N 2001 Landslide tsunami. J. Geophys. Res. 106, 11201–11215.
Baldock, J.W., 1982. Geology of Ecuador: explanatory bulletin of the national geological map of the Republic of Ecuador; 1: 1,000,000 scale. Ministerio de Recursos Naturales y Energéticos, Dirección General de Geología y Minas, Quito, Ecuador: 54pp
Bardet, J.P., Synolakis, C.E., Davies, H.L., Imamura, F. and Okal, E.A., 2003. Landslide tsunamis: Recent findings and research directions. Birkhäuser Basel: 1793-1809.
Beck, S.L. and Ruff, L.J., 1984: The rupture process of the great 1979 Colombia earthquake: evidence for the asperity model. J.Geophys. Res., 89: 9281–9291
Bender, B. (1983): Maximum likelihood estimation of b values for magnitude grouped data, Bull. Seismol. Soc. Am., 73: 831-851
Berninghausen, W.H., 1962. Tsunamis reported from the west coast of South America 1562-1960. Bull. of the Seismological Soc. of America, 52 (4): 915-921.
Biblioteca del Congreso Nacional de Chile. 2010. Efectos Económicos del Terremoto en Chile, por sectores y enel empleo: Una evaluación preliminar. BCN Informe, Santiago, Chile: 7pp.
Bristow, C.R. and Hoffstetter, R., 1977. Lexique Stratigraphique International; Ecuador. Second edition. Paris: Centre National de la Recherche Scientifique: 412p
Bryant, E., 2014. Tsunami: the underrated hazard. Springer: 222pp
Butler, R., Stewart, G.S. and Kanamori, H., 1979. The July 27, 1976 Tangshan, China earthquake—a complex sequence of intraplate events. Bulletin of the Seismological Society of America, 69(1): 207-220.
Cavallo, E.A., Powell A. and Becerra, O. 2010: Estimating the Direct Economic Damage of the Earthquake in Haiti.IDB Working Paper Series No.IDB-WP-163. The Inter American Development Bank; Department of Research and Chief Economist. Washington DC. 16 pp.
Chen, Y. ed., 1988. The great Tangshan earthquake of 1976: an anatomy of disaster. Pergamon: 162pp
Chunga, K., Besenzon, D., Mulas, M., Loayza, G. and Pindo JC., 2016: Areal distribution of Ground effects induced by the 2016 Mw 7.8 Pedernales earthquake (Ecuador). 88° Congresso della Societa' Geologica Italiana. S1. Earthquakes and Active Tectonics: a multidisciplinary approach. Napoli, 7/9 sept.
Chunga, K. and Toulkeridis, T. (2014). First evidence of paleo-tsunami deposits of a major historic event in Ecuador. J. Tsunami Soc. Int, 33: 55-69.
Collot, J.-Y., Michaud, F., Alvarado, A., Marcaillou, B., Sosson, M., Ratzov, G., Migeon, S., Calahorrano, A. and Pazmino, A., 2010. Vision general de la morfologa submarina del margen convergente de Ecuador-Sur de Colombia: implicaciones sobre la transferencia de masa y la edad de la subduccion de la Cordillera de Carnegie, in Sintesis de los Resultados de Investigacion Geologica y Geofisica Sobre el Margen Ecuatoriano, la Costa, la Cordillera Submarina de Carnegie, y de la Plataforma Volcanica de Galapagos, eds Collot, J.-Y., Sallares, V. & Pazmio, A., Publicacion CNDM-INOCAR-IRD, PSE001-09, Guayaquil, Ecuador: 47–74.
Collot, J.-Y., Michaud, F., Legonidec, Y., Calahorrano, A., Sage, F., Alvarado, A. & el personal cientifico y tecnico del INOCAR, 2005. Mapas del margen continental centro y sur de Ecuador: Bathymetria, relieve, refllectividad acustica e interpretacion geologica, Publicacion IOA - CVM- 04 - POST.

Collot, J.Y., Marcaillou, B., Sage, F., Michaud, F., Agudelo, W., Charvis, P., Graindorge, D., Gutscher, M.A. and Spence, G., 2004. Are rupture zone limits of great subduction earthquakes controlled by upper plate structures? Evidence from multichannel seismic reflection data acquired across the northern Ecuador–southwest Colombia margin. Journal of Geophysical Research: Solid Earth, 109(B11).

CRED (Centre for Research on the Epidemiology of Disasters) 2016: http://www.cred.be/node/1516

Driscoll, N.W., Weissel, J.K. and Goff, J.A., 2000. Potential for large-scale submarine slope failure and tsunami generation along the US mid-Atlantic coast. Geology, 28(5), pp.407-410.

Egbue, O. and Kellogg, J., 2010: Pleistocene to Present North Andean "escape". Tectonophysics 489: 248-257.

El Telegrafo, 2016: http://www.eltelegrafo.com.ec/noticias/ecuador/3/manana-se-daran-a-conocer-cifras-oficiales-del-costo-del-terremoto

El Universo, 2016: http://www.eluniverso.com/noticias/2016/04/25/nota/5544318/multilaterales-paises-ong-envian-recursos-exterior

Feininger, T. 1980. La geología histórica del Cretácico y el Paleógeno de la Costa Ecuatoriana, Politécnica, Monograf. Geología, V, 2: 7-48.

Ferris E. and Petz D. 2012. The year shock the rich: A review of natural disasters in 2011. Project on Internal Displacement, The Brookings Institution-The London School of Economics. Washington DC. 142 pp.

Fine I.V, Rabinovich A.B, Bornhold B.D, Thomson R.E, Kulikov E.A 2005 The Grand Banks landslide-generated tsunami of November 18, 1929: preliminary analysis and numerical modelling. Mar. Geol. 215, 45–57

Gang, Q., 1989: The Great China Earthquake. Beijing: Foreign Languages Press. 354pp

GEER-ATC Report (GEER-049), Nikolaou, S., Vera-Grunauer, X., Gilsanz, R. eds., "2016 Ecuador GEER-ATC Report version 1". Published in geerassociation.org: http://www.geerassociation.org/component/geer_reports/?view=geerreports&id=77&layout=default

Ghobarah, A., Saatcioglu, M. and Nistor, I., 2006. The impact of the 26 December 2004 earthquake and tsunami on structures and infrastructure. Engineering structures, 28(2): 312-326.

Gupta, H.K., Rao, N.P., Rastogi, B.K. and Sarkar, D., 2001. The deadliest intraplate earthquake. Science, 291(5511): 2101-2102.

Gusiakov, V.K., 2005: Tsunami generation potential of different tsunamigenic regions in the Pacific. Marine Geology, 215, 1-2: 3-9.

Gutenberg, B., 1939. Tsunamis and earthquakes. Bulletin of the Seismological Society of America, 29(4): 517-526.

Gutscher, M.A., Malavieille, J.S.L. and Collot, J.-Y., 1999: Tectonic segmentation of the North Andean margin: impact of the Carnegie ridge collision. Earth Planet. Sci. Lett. 168: 255–270.

Hampton M.A, Lee H.J, Locat J 1996 Submarine landslides. Rev. Geophys. 34: 33–59.

Harpp, K. S. and White, W. M., 2001: Tracing a mantle plume: Isotopic and trace element variations of Galápagos seamounts. Geochemistry, Geophysics, Geosystems, 2(6).

Harpp, K. S., Fornari, D. J., Geist, D. J. and Kurz, M. D., 2003: Genovesa Submarine Ridge: A manifestation of plume-ridge interaction in the northern Galápagos Islands. Geochemistry, Geophysics, Geosystems, 4(9).

Heezen B.C, Ewing M 1952 Turbidity currents and submarine slumps, and the 1929 Grand Banks Earthquake. Am. J. Sci. 250: 775–793.

Holden, J. C. and Dietz, R. S. (1972). Galapagos gore, NazCoPac triple junction and Carnegie/Cocos ridges. Nature, 235: 266-269.

Holzer, T.L. and Savage, J.C., 2013. Global earthquake fatalities and population. Earthquake Spectra, 29(1): 155-175.

Hou, J.J., Han, M.K., Chai, B.L. and Han, H.Y., 1998. Geomorphological observations of active faults in the epicentral region of the Huaxian large earthquake in 1556 in Shaanxi Province, China. Journal of structural geology, 20(5): 549-557.

Insurance Information Institute, 2016, Earthquakes and Tsunamis, Insurance Information Institute Insurance topics, from: http://www.iii.org/fact-statistic/earthquakes-and-tsunamis

International Monetary Fund. 2016. Ecuador and the IMF. Country Info August 8 2016. International Monetary Fund, Washington DC: https://www.imf.org/external/country/ECU/index.htm

IGEPN (Instituto Geofísico Escuela Politécnica Nacional), 2016a: Informe Sísmico Especial Nº 22, 2016. www.igepn.edu.ec/servicios/noticias/1341-informe-sismico-especial-n-22-2016

IGEPN (Instituto Geofísico Escuela Politécnica Nacional), 2016b: Earthquake Overview. www.igepn.edu.ec

Ioualalen, M., Ratzov, G., Collot, J.Y. and Sanclemente, E., 2011. The tsunami signature on a submerged promontory: the case study of the Atacames Promontory, Ecuador. Geophysical Journal International, 184(2): 680-688.

Kahn, M.E., 2005. The death toll from natural disasters: the role of income, geography, and institutions. Review of economics and statistics, 87(2): 271-284.

Kanamori, H. and McNally, K.C., 1982. Variable rupture mode of the subduction zone along the Ecuador-Colombia coast. Bulletin of the Seismological Society of America, 72(4): 1241-1253.

Kelleher, J.A., 1972: Ruptures zones of large South American earthquakes and some predictions. Journal of Geophysical Research, 77, 11: 2087-2103.

Kellogg, J.N. and Vega, V., 1995: Tectonic development of Panama, Costa Rica and the Colombian Andes: Constraints from Global Positioning System geodetic studies and gravity. Geol. Soc. Am. Special Paper 295: 75–90.

Lebrat, M., Megard, F., Dupuy, C and Dostal, J., 1987: Geochemistry and tectonic setting of pre-collision Cretaceous and Paleogene volcanic rocks of Ecuador. Bulletin of the geological society of America, 99: 569-578.

Marano, K.D., Wald, D.J. and Allen, T.I., 2010. Global earthquake casualties due to secondary effects: a quantitative analysis for improving rapid loss analyses. Natural hazards, 52(2): 319-328.

Martínez, S. and El Comercio DATA. 2016: Conozca 208 bienes y servicios que pagarán 14% de IVA en Ecuador. Sección El Comercio-DATA, Compañía Anómima El Comercio, Quito, Ecuador. http://www.elcomercio.com/datos/servicios-productos-aumento-iva-ecuador.html

Masson, D.G., Harbitz, C.B., Wynn, R.B., Pedersen, G. and Løvholt, F., 2006: Submarine landslides: processes, triggers and hazard prediction. Philosophical Transactions of the Royal Society of London A: Mathematical, Physical and Engineering Sciences, 364(1845): 2009-2039.

McAdoo, B.G. and Watts, P., 2004: Tsunami hazard from submarine landslides on the Oregon continental slope. Marine Geology, 203(3): 235-245.

McCaffrey, R., 2008. Global frequency of magnitude 9 earthquakes. Geology, 36(3): 263-266.

McGuire, R.K., 1995. Probabilistic seismic hazard analysis and design earthquakes: closing the loop. Bulletin of the Seismological Society of America, 85(5): 1275-1284.

Michetti A.M., Esposito E., Guerrieri L., Porfido S., Serva L., Tatevossian R., Vittori E., Audemard F., Azuma T., Clague J., Comerci V., Gürpinar A., McCalpin J., Mohammadioun B., Mörner N.A., Ota Y. and Rogozhin E., 2007:. Intensity Scale ESI 2007. La Scala di Intensità ESI 2007, ed. L. Guerrieri e E. Vittori (Memorie Descrittive della Carta Geologica d'Italia, vol.74, Servizio Geologico d'Italia – Dipartimento Difesa del Suolo, APAT), Roma, http://www.apat.gov.it/site/it-IT/Progetti/-INQUA_Scale/.

Papanikolaou, I.D., Foumelis, M., Parcharidis, I., Lekkas, E.L. and Fountoulis, I.G., 2010: Deformation pattern of the 6 and 7 April 2009, MW= 6.3 and MW= 5.6 earthquakes in L'Aquila (Central Italy) revealed by ground and space based observations. Nat. Hazards Earth Syst. Sci, 10(1): 73-87.

Pararas-Carayannis, G. 1980: The Earthquake and Tsunami of December 12, 1979, in Colombia. Intern. Tsunami Information Center Report, Abstracted article in Tsunami Newsletter, Vol. XIII, No. 1.

Pararas-Carayannis, G., 1967: A study of the source mechanism of the Alaska earthquake and tsunami of March 27, 1964: Part I, Water waves. Pacific Science, 21: 301-310.

Pararas-Carayannis, G., 2006: The potential of tsunami generation along the Makran Subduction Zone in the northern Arabian Sea: Case study: The earthquake and tsunami of November 28, 1945. Science of Tsunami Hazards, 24(5): 358-384.

Pararas-Carayannis, G., 2010: The earthquake and tsunami of 27 February 2010 in Chile–Evaluation of source mechanism and of near and far-field tsunami effects. Science of Tsunami Hazards, 29, 2: 96-126.

Pararas-Carayannis, G., 2012: Potential of tsunami generation along the Colombia/Ecuador subduction margin and the Dolores-Guayaquil Mega-Thrust. Science of Tsunami Hazards, 31, 3: 209-230.

Pararas-Carayannis, G., 2014. The Great Tohoku-Oki earthquake and tsunami of March 11, 2011 in Japan: A critical review and evaluation of the tsunami source mechanism. Pure and applied geophysics, 171(12): 3257-3278.

Parra, H; Benito, B, Gaspar-Escribano, J. (2016). Seismic Hazard Assessment in Continental Ecuador. Bull Earthquake Eng., 1-31. DOI 10.1007/s10518-016-9906-7

Pilger, R. H., 1983. Kinematics of the South American subduction zone from global plate reconstructions. Geodynamics of the eastern Pacific region, Caribbean and Scotia arcs: 113-125.

Pontoise, B. and Monfret, T. (2004). Shallow seismogenic zone detected from an offshore‐onshore temporary seismic network in the Esmeraldas area (northern Ecuador). Geochemistry, Geophysics, Geosystems, 5(2).

Raschky, P.A. 2008. Institutions and the losses from natural disasters. Natural Hazards and Earth System Science 8: 627-634.

Ratzov, G., Collot, J. Y., Sosson, M. and Migeon, S. (2010). Mass-transport deposits in the northern Ecuador subduction trench: Result of frontal erosion over multiple seismic cycles. Earth and Planetary Science Letters, 296(1): 89-102.

Ratzov, G., Sosson, M., Collot, J. Y., Migeon, S., Michaud, F., Lopez, E. and Le Gonidec, Y. (2007). Submarine landslides along the North Ecuador–South Colombia convergent margin: possible tectonic control. In Submarine Mass Movements and Their Consequences. Springer Netherlands: 47-55

Reyes, P & Michaud, F, 2012 "Mapa Geológico de la Margen Costera Ecuatoriana", 1:500.000. Petroecuador – EP – IRD (Eds). Quito Ecuador.

Reynaud, C., Jaillard, É., Lapierre, H., Mamberti, M. and Mascle, G. H. (1999). Oceanic plateau and island arcs of southwestern Ecuador: their place in the geodynamic evolution of northwestern South America. Tectonophysics, 307(3): 235-254.

Rodriguez, F., DHowitt, M.C., Toulkeridis, T., Salazar, R., Romero, G.E.R., Moya, V.A.R. and Padilla, O., 2016. The economic evaluation and significance of an early relocation versus complete destruction by a potential tsunami of a coastal city in Ecuador. Journal of Tsunami Society International, 35(1). 18-35

Rudolph E. and Szirtes S., 1911: Das kolumbianische Erdbeben am 31 Januar 1906, Gerlands Beitr. z. Geophysik , 2: 132- 275.

Ruff, L.J., and Kanamori, H., 1980, Seismicity and the subduction process: Physics of the Earth and Planetary Interiors, v. 23: 240–252, doi: 10.1016/0031–9201(80)90117-X.

Sato, H., Fehler, M.C. and Maeda, T., 2012. Seismic wave propagation and scattering in the heterogeneous earth, Berlin: Springer. 496pp

Secretaria Nacional de Gestión de Riesgos-SNGR. 2016. Informe de Siatuación No. 71. Equipo Técnico de la Secretaría de Gestión de Riesgos, SNGR. 15 pp. http://www.gestionderiesgos.gob.ec/wp-content/uploads/downloads/2016/05/INFORME-n71-SISMO-78-20302.pdf

Senplades. 2016. Evaluación de los Costos de Reconstrucción Sismo en Ecuador, abril 2016.Secretaría Nacional de Planificación y Desarrollo - Senplades, Quito, Ecuador. 20 pp.

Shepperd, G.L. and Moberly, R., 1981: Coastal structure of the continental margin, northwest Peru and southwest Ecuador. Geological Society of America Memoirs, 154: 351-392,

Shome, N., Cornell, C.A., Bazzurro, P. and Carballo, J.E., 1998. Earthquakes, records, and nonlinear responses. Earthquake Spectra, 14(3): 469-500.

Sieh K 2005 Aceh-Andaman earthquake: What happened and what's next?. Nature. 434: 573–574

Stainforth, R.M. 1948. Applied micropaleontology in Coastal Ecuador, Jour. Paleontology, 22, 142-146.

Swenson, J.L. and Beck, S.L., 1996: Historical 1942 Ecuador and 1942 Peru subduction earthquakes, and earthquake cycles along Colombia–Ecuador and Peru subduction segments. Pure Appl. Geophys.146 (1): 67–101.

Synolakis, C.E., Bardet, J.P., Borrero, J.C., Davies, H.L., Okal, E.A., Silver, E.A., Sweet, S. and Tappin, D.R., 2002, April. The slump origin of the 1998 Papua New Guinea tsunami. In Proceedings of the Royal Society of London A: Mathematical, Physical and Engineering Sciences, Vol. 458, No. 2020: 763-789.

Tappin, D.R., Watts, P., McMurtry, G.M., Lafoy, Y., Matsumoto, T., 2001. The Sissano Papua New Guinea tsunami of July 1998 - ofshore evidence on the source mechanism. Mar. Geol. 175, 1-23; Nature 379(18): 246-249.

Tappin, D.R., Watts, P., McMurtry, G.M., Lafoy, Y., Matsumoto, T., 2002. Prediction of slump generated tsunamis: The July 17, 1998 Papua New Guinea event. Sci. Tsunami Hazards 20: 222-238.

The World Bank. 2016. Ecuador Overview. World Bank – Ecuador home. Washington DC: http://www.worldbank.org/en/country/ecuador/overview

Tierra, A., Toulkeridis, T., Sani, J., Padilla Almeida, O. and Parra, H., 2017: Evaluation of horizontal and vertical positions obtained from an unmanned aircraft vehicle applied to large scale cartography of Infrastructure loss due to the Earthquake of April 2016 in Ecuador. Journal of Disaster Research, in press

Tinti, S., Armigliato, A., Pagnoni, G. and Zaniboni, F., 2005. Scenarios of giant tsunamis of tectonic origin in the Mediterranean. ISET Journal of Earthquake Technology, 42(4): 171-188.

Toulkeridis et al., 2017b; Real-Time Radioactive Precursor of the April 16, 2016 Mw 7.8 Earthquake in Ecuador. Submitted

Toulkeridis, T., Parra, H., Mato, F., Cruz D´Howitt, M., Sandoval, W., Padilla Almeida, O., Rentería, W., Rodríguez Espinosa, F., Salazar martinez, R., Cueva Girón, J., Taipe Quispe, A. and Bernaza Quiñonez, L., 2017a: Contrasting results of potential tsunami hazards in Muisne, central coast of Ecuador. J. Tsunami Soc. Int, 36: 13-40.

Toulkeridis, 2011: Volcanic Galápagos Volcánico. Ediecuatorial, Quito, Ecuador: 364 pp

Tschopp, H.J. 1953. Oil exploration in the Oriente of Ecuador. Bull.AAPG, 37: 2303-2347.

UNISDR, Corporación OSSO, 2016: Impacto de los desastres en América latina y el Caribe 1990-2013: Tendencias y estadísticas para 22 países. Oficina de las Naciones Unidas para la Reducción del Riesgo de Desastres-INISDR, Agencia Española de Cooperación Internacional para el Desarrollo-aecid, Corporación OSSO: 70 pp.

USGS (United States Geological Service), 2016a: Historic Earthquakes, 1906 January 31st. (http://earthquake.usgs.gov/earthquakes/world/events/1906_01_31.php)

USGS (United States Geological Service), 2016b: M7.8 - 29km SSE of Muisne, Ecuador.http://earthquake.usgs.gov/earthquakes/eventpage/us20005j32#general

USGS (United States Geological Service), 2016c: Earthquake Glossary - aftershocks.https://earthquake.usgs.gov/learn/glossary/?term=aftershocks

USGS (United States Geological Service), 2016d: Earthquake Catalog Search.https://earthquake.usgs.gov/earthquakes/search/

Ward S.N 2001 Landslide tsunami. J. Geophys. Res. 106, 11201–11215.